

Structural Modifications that Alter the P-Glycoprotein Efflux Properties of Compounds

Stephen A. Hitchcock[†]

Envoy Therapeutics, 555 Heritage Drive, Jupiter Florida 33458, United States

1. INTRODUCTION

Retrospective analysis of marketed drugs has revealed that very low prevalence of P-glycoprotein (P-gp) efflux and moderate to high passive permeability are two key properties that distinguish drugs which engage targets in the central nervous system (CNS) from those that act predominantly in the periphery. Quantification of the efflux properties that differentiate CNS drugs has been determined using *in vitro* assays for human and rodent P-gp,^{1,2} and revealed *in vivo* by comparing brain drug exposures in P-gp (*mdr1a/b*^(-/-)) knockout mice against those observed in wild type mice.³ Recognition by P-gp not only dramatically affects the distribution properties of compounds into bodily compartments including the CNS, testis, and placenta but also confers resistance to certain cancer chemotherapeutics. This perspective is focused on structural modifications and strategies that can be applied during compound optimization in order to modulate the P-gp efflux properties of small molecules with a particular emphasis on implications for CNS penetration. The topic was last reviewed in 2006 by Raub⁴ who noted at the time a surprising paucity of published examples where P-gp efflux had been purposefully circumvented. Greater awareness of the implications of efflux coupled with advances in the quality and throughput of *in vitro* permeability and efflux assays,⁵ greater access to genetic mouse models that lack expression of P-gp,^{6,7} and the development of tool compounds that inhibit efflux transporters⁸ has led to an improved understanding of how structural properties influence efflux recognition. However, the precise molecular interactions that confer P-gp efflux remain relatively poorly defined. The promiscuous nature of P-gp renders the rational circumvention of efflux, while simultaneously optimizing compounds for efficacy, safety, and pharmacokinetic properties, an extremely challenging undertaking.

The sequence of the human genome has revealed that 500–1200 genes encode for transport proteins.⁹ Energy-dependent active transport proteins are utilized to varying degrees by all cells to traffic a wide variety of substrates including ions, small molecules, and macromolecules against concentration gradients spanning extra- and intracellular biological membranes. Active uptake proteins control the translocation of molecules required for healthy cellular function, whereas efflux transporters serve to expel endogenous and exogenous molecules that are recognized as being potentially harmful. Eukaryotic transmembrane transport proteins have been categorized into several subclasses,¹⁰ the two largest being the solute carrier class (SLC) with 348 members identified, and the ATP-binding cassette (ABC) family containing 7 subfamilies (A–G) and 48 identified members.¹¹ Three ABC proteins; P-gp (encoded by ABCB1 (MDR1)), multidrug resistance protein 1 (MRP1 encoded by ABCC1), and breast cancer resistance protein

(BCRP encoded by ABCG2) confer resistance to tumor cells and consequently are among the most extensively studied of the ABC family members. In addition to their role in cancer chemotherapy resistance, P-gp, MRPs, and BCRP also have a significant influence on the absorption, clearance, and penetration of a vast array of small molecules into specific cellular and tissue compartments. P-gp was the first human ABC transporter to be cloned and has been the most extensively studied.¹² P-gp is a glycosylated membrane protein of 170 kDa, and is broadly expressed but particularly enriched in the intestines, liver, kidneys, and at the blood–brain barrier (BBB) and blood–cerebrospinal fluid barrier (BCSFB). P-gp is a highly permissive transporter, recognizing and effluxing a vast diversity of small molecules and peptides. At least 15 additional efflux transporters including members from the organic anion transporter (OAT), multidrug resistance-associated protein (MRP), multidrug resistance protein (MDR), and organic anion transporting polypeptide (OATP) families have been detected at the BBB at the mRNA level.¹³ However, P-gp has assumed prominence primarily due to the fact that it has been confirmed experimentally as possessing the broadest substrate specificity.

2. SIGNIFICANCE OF P-GP EFFLUX IN DRUG DESIGN

The quantitative effect of P-gp efflux on intestinal absorption is generally much lower than that affecting entry into the CNS due to the fact that drug plasma concentrations rarely reach saturating levels at the BBB. However, particularly for low dose drugs, oral bioavailability and clearance can be altered by P-gp and can lead to drug–drug interactions (DDIs) and inter-patient variability. Several single nucleotide polymorphisms (SNPs) for P-gp have been documented and shown to influence the pharmacokinetics of drugs (e.g., digoxin). For example, a SNP in exon 26 of the MDR1 gene, C3435T, has been identified within ethnic groups and correlated with diminished expression levels of P-gp.¹⁴ Individuals homozygous for the T allele have a greater than 4-fold decrease in P-gp expression levels compared with that of CC individuals. The C3435T allele has also been associated with an increased risk of Parkinson's disease in individuals exposed to neurotoxic pesticides.¹⁵ The fact that MDR1 SNPs are associated with altered oral bioavailability and clearance of P-gp substrates must be considered if a strategy to minimize CNS penetration by engineering in P-gp efflux to compounds is pursued.

It is worthwhile mentioning some complicating aspects of P-gp function that relate to the translation from preclinical models to the human clinical setting. P-gp activity and expression can be modulated by a variety of pharmacological, physiological,

Received: August 24, 2011

Published: April 16, 2012

and pathological stresses resulting in either increases or decreases in transport activity. The BBB has been shown to possess a remarkable capacity to regulate the expression of P-gp in order to maintain homeostasis.¹⁶ P-gp is dynamically regulated at the transcriptional level by promoter elements such as constitutive androstane receptor, nuclear factor- κ B, activator protein-1, and particularly by pregnane X receptor (PXR in rodents and SXR (steroid and xenobiotic receptor) in humans).¹⁷ Further complicating matters, the PXR/SXR ligand-binding domains display substantially different ligand affinities between the rodent and human homologues.¹⁸ Pharmacoresistance in several CNS disorders including schizophrenia¹⁹ and epilepsy,²⁰ in both human subjects and in animal models, has been linked to increased P-gp activity.²¹ Upregulation of P-gp likely contributes to the development of resistance to several drugs including morphine. For example, brain P-gp, as measured by Western blot analysis, has been shown to increase approximately 2-fold in rats chronically treated with morphine, which is a substrate for the transporter.²²

There is also evidence that P-gp expression levels can be altered in disease models. For example, λ -carrageenan-induced peripheral inflammatory hyperalgesia in the rat has been shown to increase P-gp expression within the brain endothelium, resulting in decreased CNS penetration of morphine and attenuation of morphine-induced antinociception.²³ Neuroinflammation associated with multiple sclerosis and Alzheimer's disease has been suggested to contribute to disruption of the BBB in humans. However, comparison of the brain penetration of eight small molecules in naive animals and the experimental autoimmune encephalomyelitis model of multiple sclerosis and in two models of Alzheimer's disease (a TASTPM transgenic model and a streptozotocin model) showed no significant differences in brain penetration.²⁴

Age-associated decline in P-gp function has been proposed as a contributing risk factor in the pathophysiology of neurodegenerative conditions such as Alzheimer's and Parkinson's diseases²⁵ and also in psychiatric disorders.²⁶ P-gp has been proposed to facilitate the expulsion of neurotoxic peptides such as Amyloid β -peptide ($A\beta$) and α -synuclein. Post-mortem analysis of brain samples from nondemented aged human subjects has revealed an inverse correlation between P-gp expression and the deposition of both $A\beta_{40}$ and $A\beta_{42}$ in the medial temporal lobe.²⁷ In addition to the age-related decrease of P-gp expression, it has recently been demonstrated in mice that $A\beta_{42}$ itself downregulates the expression of P-gp in addition to other $A\beta$ transporters. This phenomenon may further exacerbate the diminished clearance of $A\beta$ from the CNS observed with aging and consequently accelerate neurodegeneration.²⁸

In summary, extrapolation of the effects of P-gp efflux on compound disposition and efficacy from in vitro and rodent models into aged and/or diseased human populations is complex and contributes to increased uncertainty.^{29,30} This further emphasizes the value of optimizing CNS drug candidates for the lack of P-gp efflux, in addition to early investment in translatable biomarkers for CNS disease programs.³¹

3. EXPERIMENTAL MEASURES OF P-GP EFFLUX

The nonfenestrated endothelium of brain capillaries that constitutes the BBB physically limits the passive permeability of compounds and also presents a metabolic barrier to CNS entry in the form of metabolizing enzymes and transport proteins. P-gp is expressed at high levels at the luminal face (blood-side) of the brain vascular endothelium in addition to

the endothelial cells of the choroid plexus where it facilitates transport toward the CSF. Human MDR1 and rodent *mdr1a/1b* gene products confer drug efflux, with rodent *mdr1a* operating at the BBB and *mdr1b* within the brain parenchyma (neurons and surrounding glial cells). Although P-gp homology at the amino acid level is high across species (87%, 85%, 87%, and 93% between human and mouse, rat, dog, and rhesus monkey, respectively), compounds that exhibit different efflux properties across species have been observed^{32,33} (vide infra). Recent in vitro data comparing the human and mouse P-gp efflux properties of 3300 Pfizer compounds suggest, however, that rodent–human divergence is a relatively rare occurrence but that it can be biased toward either species (Figure 1).¹

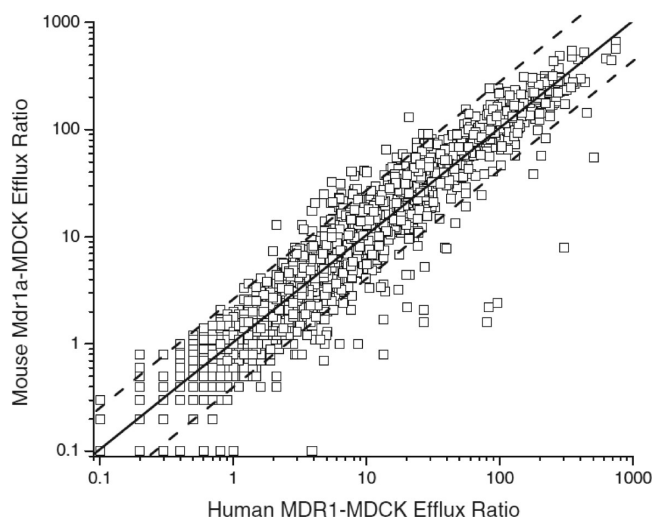


Figure 1. Correlation of the efflux ratio in transwell assays using mouse *Mdr1a*-MDCK and human MDR1-MDCK cells for 3300 Pfizer compounds. The y-axis is the mouse *Mdr1a*-MDCK efflux ratio, and the x-axis is the human MDR1-MDCK efflux ratio. $R^2 = 0.92$. The solid line is the linear regression line, and the dotted line is the 95% prediction interval. Reprinted with permission from ref 1. Copyright 2008 ASPET Publications.

In vivo models and in vitro assays^{34,35} for assessing P-gp efflux have been reviewed elsewhere, so only brief mention of key factors will be made here. Substrate inhibition assays using cellular uptake of rhodamine-123 or calcein AM, functional assays measuring ATPase activity, and transcellular transport assays have been utilized for the measurement of P-gp activity. Transwell-based assays using polarized cell lines such as the Madin–Darby canine kidney (MDCK) and pig-kidney-derived epithelial (LLC-PK) cell lines have become the favored in vitro assays for assessing P-gp efflux and have provided a large amount of the data discussed in this review. The MDCK and LLC-PK cell lines have become particularly popular as they possess relatively low background expression of endogenous transporters and can be stably transfected with human MDR1 or rodent *mdr1a* (MDR1-MDCK or *Mdr1a*-MDCK, respectively). It should be noted, however, that the MDCK cell line does express a number of endogenous transport proteins, and recently, it has been asserted that the contribution of these transporters to compound permeability has been underestimated.³⁶ Apical-to-basal (A-B) versus basal-to-apical (B-A) permeability rates are used to define the efflux ratio (ER), and generally, cutoff values from 1.5 to 3 are used to distinguish P-gp substrates from nonsubstrates. As mentioned previously,

moderate to high passive permeability is highly desired for CNS targeted agents. Moderate A-B permeability in parental MDCK and LLC-PK assays is considered to reside in the 10 to 15×10^{-6} cm/s range with A-B $> 15 \times 10^{-6}$ cm/s considered to be high permeability.³⁷ There is some evidence that high passive permeability can somewhat counteract the effects of moderate P-gp efflux in vivo. Given its lower cost, higher throughput, and absence of transport proteins, the parallel artificial membrane permeability assay (PAMPA) adapted for BBB (PAMPA-BBB)³⁸ can be positioned in testing cascades as a filter assay to select compounds with sufficient passive permeability to test in P-gp efflux assays. The impact of P-gp in vivo can be assessed by comparing the exposure of compounds in wild type *mdr1a*^(+/+) versus *mdr1a*^(-/-) knockout mice.³⁹ Alternatively, a number of small molecule P-gp inhibitors such as elacridar,⁴⁰ pantoprazole, and cyclosporine have been used to create “chemical” P-gp knockouts with the advantage that these expand the scope of studies into species beyond mice.⁴¹ It must be borne in mind, however, that these compounds also inhibit other transporters including BCRP, and recently, mice with a double knockout of *mdr1a/b*^(-/-)/*Bcrp*^(-/-) have revealed a synergistic role between these two efflux proteins.⁴²

It is now generally accepted that employing total drug brain-to-plasma (B/P) ratios from in vivo experiments is an unreliable and often misleading gauge of pharmacologically relevant drug exposure in the CNS. Over the past few years, integrative models have been developed based on the free-drug hypothesis that utilizes unbound drug levels in brain and plasma ($f_{u,brain}/f_{u,plasma}$) and CSF drug levels as more relevant measures that more accurately predict biological target engagement.^{43–45} However, it should be noted that CSF drug levels can overestimate unbound brain concentrations for P-gp substrates due to the lower efflux capacity of the blood–cerebrospinal fluid barrier compared to the blood–brain barrier.⁴⁶ Modern approaches for optimizing the pharmacokinetic properties of compounds for CNS activity incorporate unbound fraction in plasma and brain and factors for passive permeability and P-gp efflux.^{47,48}

4. COMPOUND DESIGN TOOLS FOR CNS EXPOSURE

Within the context of modern integrative approaches to optimizing for compounds for CNS activity, it is well recognized that compound physicochemical properties have a profound influence on nonspecific binding to plasma proteins and tissue, passive permeability, and efflux in addition to other important ADMET properties.⁴⁹ Despite the lore that compound lipophilicity is correlated with brain exposure, LogP is not correlated with brain unbound drug levels, the true determinant of pharmacologically relevant exposure. Molecular descriptors related to hydrogen bonding (topological polar surface area (tPSA), hydrogen bond donor count (HBD), and hydrogen bond acceptor count (HBA)) in fact dominate the relationship with $K_{p,uu,brain}$, the steady-state unbound brain-to-plasma concentration ratio.⁵⁰ This finding is likely due to the additive effect that PSA, HBD, and HBA have on simultaneously reducing passive permeability while increasing the probability of interactions with efflux transporters. This posit is supported by analysis of the physicochemical properties of 4176 compounds from Amgen medicinal chemistry projects and their in vitro passive permeability measured in a parental LLC-PK assay and human P-gp efflux measured in an MDR1-LLC-PK assay (Figure 2). These data reveal a dominant role of tPSA and particularly HBD count on the average P-gp efflux ratio. For

example, 52% of compounds tested with tPSA $> 90 \text{ \AA}^2$ were categorized as P-gp efflux substrates (ER > 3), whereas only 14% of the compounds with tPSA $< 70 \text{ \AA}^2$ were considered P-gp efflux substrates. A similar trend is evident from HBD count, with 57% of compounds possessing > 2 HBDs vs 9% with zero HBD being classified as P-gp efflux substrates. CLogP, however, had little influence on P-gp efflux and did not overly negatively impact passive permeability until values well outside acceptable oral drug-like ranges were reached (CLogP < 1 or > 7). These data support previously recommended guidelines of maintaining tPSA $< 90 \text{ \AA}^2$ and HBD < 2 to maximize the probability of evading P-gp efflux.⁵¹

Researchers at Pfizer have recently developed an algorithm termed central nervous system multiparameter optimization (CNS MPO) employing combined weightings from six physicochemical parameters (clogP, clogD, tPSA, MW, HBD, and pK_a).⁵² Analysis of a large diverse set of Pfizer compounds used to develop the algorithm also revealed that there is little correlation between clogP and P-gp efflux liability in a MDCK-MDR1 assay and that only when cLogP exceeded 5 was an increase in P-gp liability observed. There appears to be a large range of tolerated cLogP values for avoidance of P-gp efflux. However, lipophilicity remains an important component of drug-likeness given its significant influence on other parameters such as pharmacological promiscuity, protein binding, and solubility and cannot be disregarded for these reasons.⁵³

Although these molecular descriptor guidelines are helpful in compound design, it is clear that compounds with identical physicochemical properties can have vastly different efflux properties due to the nature and presentation of functionality in the molecule. P-gp after all depends on a small molecule protein interaction. However, unlike the typical small molecule–drug target interaction, P-gp is a highly permissive protein recognizing a wide diversity of substrates. The rule-of-thumb guidelines are helpful in reducing the probability of encountering P-gp efflux and prioritizing modifications for its mitigation but also highlight the necessity for frequent assaying of compounds and experimentally driven, precision-guided optimization.

The potential for improved structure-based approaches for modulation of P-gp activity has arrived with the recent publication of the mouse P-gp apo crystal structure at 3.8 \AA resolution along with two cocrystal structures with enantiomers of a cyclic peptide P-gp inhibitor.⁵⁴ The X-ray structure revealed that protein is arranged in a folded conformation with pseudo 2-fold symmetry, an internal cavity of $\sim 6000 \text{ \AA}^3$ with a very large hydrophobic substrate binding domain, and two nucleotide-binding domains (Figure 3). The protein structure supports a “hydrophobic vacuum cleaner” model whereby large openings to the cytoplasm and the inner leaflet of the lipid bilayer are used for compound entry, but substrate access is blocked from the outer membrane leaflet and the extracellular compartment (Figure 4). Thus, compounds must be sufficiently membrane permeable to be accessed by P-gp which scans for substrates by sampling a wide cross section of conformations. Once bound to the protein, substrate then induces binding of two molecules of ATP triggering a large conformational shift resulting in an outward-facing cavity and ejection of the substrate into the extracellular space. Hydrolysis of ATP then returns the protein back to its inward facing drug binding conformation and reinitiates the transport cycle. Examples whereby structure-based design results in rational modification of P-gp-compound recognition are eagerly awaited. However, the limited resolution of

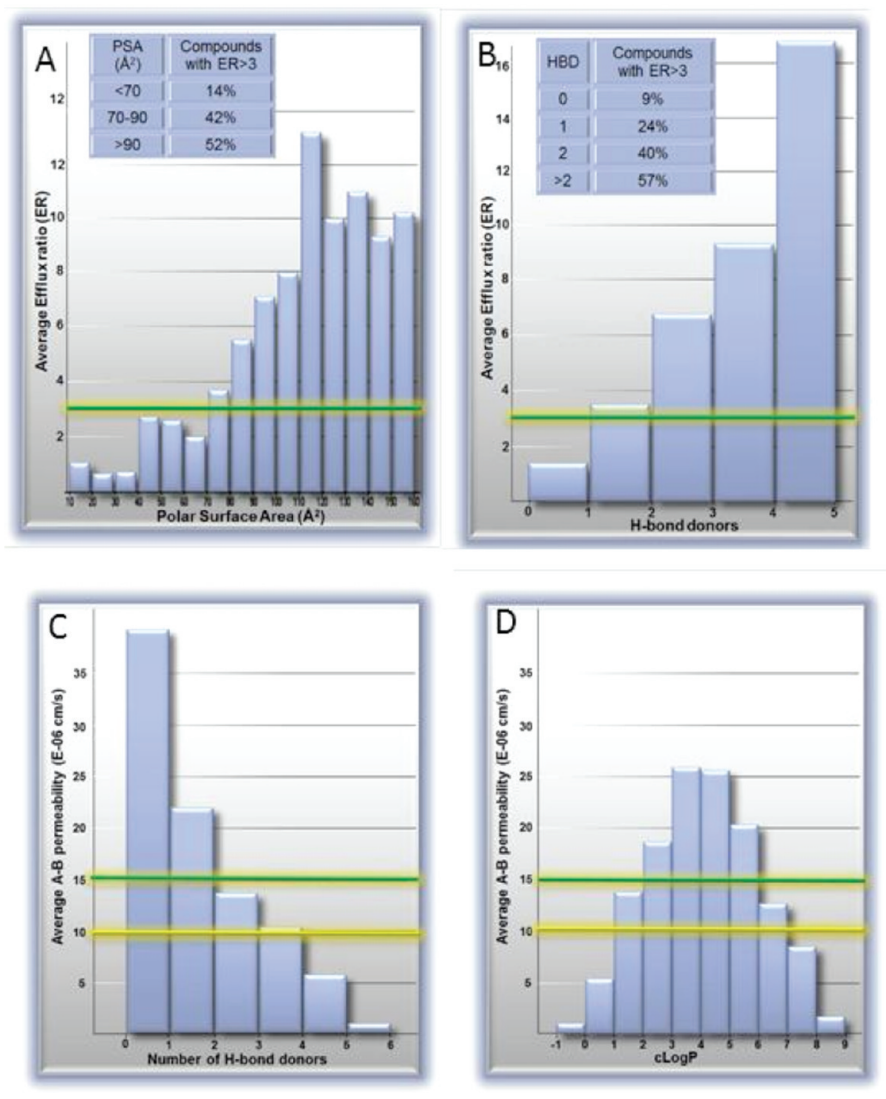


Figure 2. Average A-B permeability and efflux ratios (ER) of 4176 Amgen compounds in an MDR1-LLC-PK cell assay. (A) Average efflux ratio and percentage of compounds defined as P-gp substrates (ER > 3) by bucketed tPSA values, (B) average efflux ratio and percentage of compounds defined as P-gp substrates (ER > 3) by bucketed hydrogen bond donor (HBD) count, (C) average A-B permeability by bucketed HBD count, and (D) average A-B permeability by bucketed cLogP values.

the available X-ray structure and the highly flexible nature of the protein will no doubt present significant challenges.⁵⁵

The sheer number of ligand-based computational models for P-gp that have been published is a reflection of the challenges posed by the high substrate promiscuity of the protein. It has been suggested that the crystal structure of P-gp supports an “induced-fit” ligand binding model that renders it particularly difficult to predict binders versus nonbinders with high accuracy.⁵⁶ Given the multiplicity of binding sites and allosteric interactions, it is unlikely that any single pharmacophore model or quantitative structure–activity relationship (QSAR) can describe the expanse of spatial arrangements and structural features responsible for P-gp recognition. The many pharmacophore models, machine-learning algorithms, and QSAR approaches have been reviewed elsewhere.⁵⁷

5. EXAMPLES OF P-GP EFFLUX MITIGATION VIA STRUCTURAL MODIFICATION

The following examples serve to illustrate a variety of relatively modest structural changes that have been utilized to modulate

P-gp efflux properties. It is a testimony to the ingenuity of chemists that, in the majority of cases described here, efforts to engineer out efflux while simultaneously maintaining biological target activity, selectivity and in many cases, favorable pharmacokinetic properties have been successful. For reference, cLogP, tPSA MW, and HBD count are included, along with calculated LogD and pK_a values where relevant, in the tables for all compounds. Compound property values were calculated using ACD/Percepta software, version 14.0 (ACD/laboratories).

5.1. Amides, Sulfonamides, and Ureas. Antagonists of the bradykinin B1 receptor, a class A peptide G-protein coupled receptor (GPCR) that is induced in response to painful stimuli or inflammation, have long been sought after as potential therapeutics for pain. P-gp efflux has plagued many of the compound series pursued as B1 antagonists despite the broad cross-section of chemical diversity represented by the scaffolds that have been explored.⁵⁸ Securing sufficient B1 antagonist potency within the confines of CNS-accessible chemical space, particularly with respect to tPSA and MW, has proven especially challenging. There have been disclosures from several

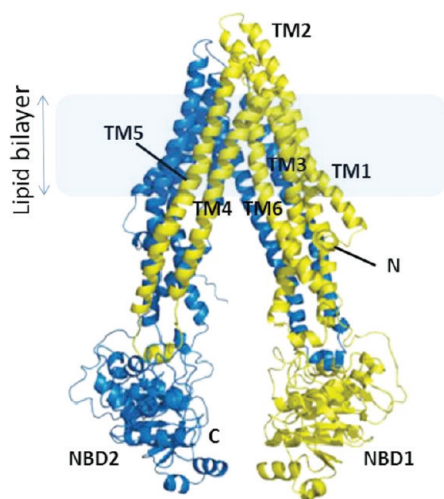


Figure 3. Crystal structure of mouse P-gp. Transmembrane (TM) regions 1–6 are labeled. The N- and C-terminal halves of the molecule are colored yellow and blue, respectively. NBD = nucleotide binding domain. The shaded area represents the approximate positioning of the lipid bilayer. The N- and C-termini are labeled. Reprinted with permission from ref 54. Copyright 2009 AAAS.

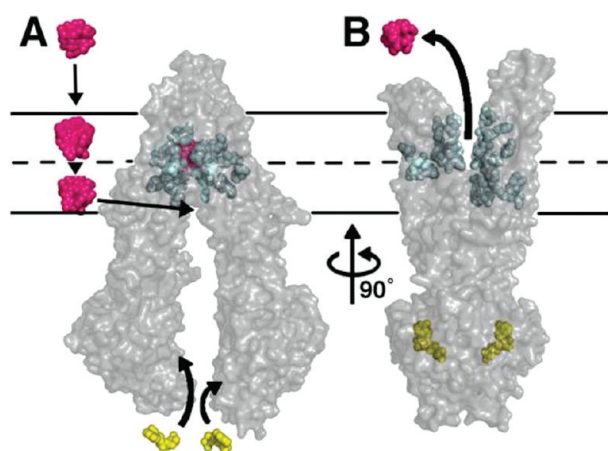


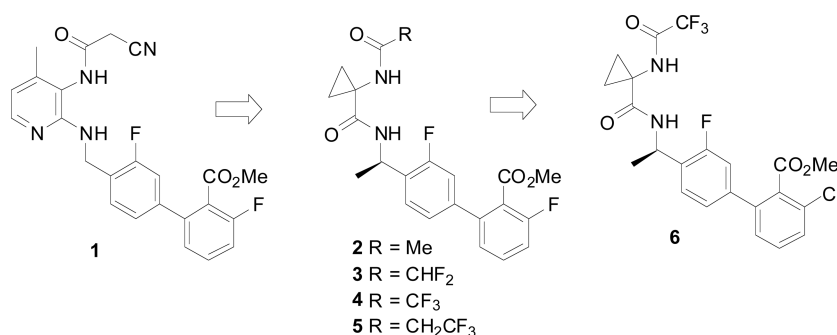
Figure 4. Model of substrate transport by P-gp. The substrate (magenta) partitions into the bilayer from outside of the cell to the inner leaflet and enters the internal drug-binding pocket through an open portal. The residues in the drug-binding pocket (cyan spheres) interact with ligands in the inward-facing conformation. ATP (yellow) binds to the two nucleotide binding domains causing a large conformational change and presenting the substrate and drug-binding site(s) to the outer leaflet and/or extracellular space. Exit of the substrate to the inner leaflet is sterically occluded, which provides unidirectional transport to the outside. Reprinted with permission from ref 54. Copyright 2009 AAAS.

groups in recent years describing efforts to balance potency, P-gp susceptibility, hERG blockade, and pharmacokinetics during B1 antagonist optimization. A notable success, resulting in the selection of cyclopropylamide **6** as a clinical development candidate, has been disclosed by researchers at Merck (Figure 5).⁵⁹ The series had its origins in diaminopyridine lead **1**, which displayed good B1 antagonist potency ($K_i = 0.71$ nM) but was determined to be a P-gp efflux substrate (ER = 22.6) as measured in an MDR1-LLC-PK assay. Replacement of the diaminopyridine moiety in **1** with a cyclopropylcarboxamide served to reduce molecular weight while preserving potency, leading to

compounds such as **2**. Although somewhat diminished relative to **1**, **2** still displayed P-gp efflux properties (ER = 8.6), although with high passive permeability ($p_{app} = 21 \times 10^{-6}$ cm/s). A remarkable attenuation of the P-gp efflux ratio was elicited by the exchange of the acetamide in **2** for either a difluoro- or trifluoroacetamide resulting in compounds **3** and **4** having ERs of 3.2 and 2.3, respectively, while maintaining subnanomolar B1 antagonist potencies and high passive permeability. The 3,3,3-trifluoropropanamide **5**, however, produced an ER of 8.6 revealing the subtle nature of the modulation of P-gp recognition. The chloro analogue **6** retained good B1 potency and a low P-gp ER of 1.9. When tested in a transgenic rat model expressing human B1 receptors, **6** demonstrated good CNS penetration achieving 90% CNS B1 receptor occupancy at a brain concentration of 520 nM. In a humanized B1 mouse model, **6** also reversed CFA-induced hyperalgesia with an ED_{50} of 9.76 mg/kg p.o. Interestingly, although not a substrate for human P-gp, **6** was found to be a substrate for mouse P-gp in vitro (ER = 9.3) and in vivo as demonstrated in P-gp knockout mice. The brain to plasma AUC ratio of **6** in P-gp knockout mice was 1.05 but was 9-fold lower in wild-type mice. It was reasoned that **6** was worthy of progression based on a low probability for human P-gp efflux, and encouragingly, **6** produced a brain to plasma ratio of 0.4 in Rhesus monkey at 2 h after a 2 mg/kg iv dose.

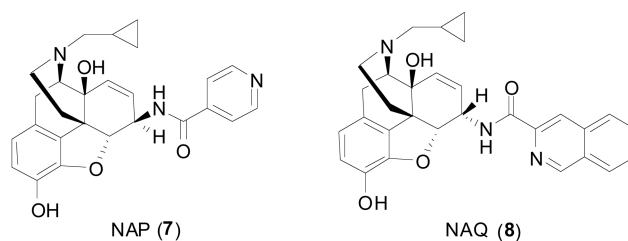
A pair of potent selective Mu opioid receptor antagonists with strikingly different efflux properties and CNS activity in vivo has recently been described⁶⁰ (Figure 6). The naltrexamine derivatives NAP (**7**) and NAQ (**8**) have similar subnanomolar potencies against the Mu receptor with very good selectivity over the other opioid receptor subtypes. However, in a mouse tail immersion test, **7** was 10-fold less potent based on dose ($AD_{50} = 4.98$ mg/kg) when compared to that of **8** ($AD_{50} = 0.46$ mg/kg) in antagonizing the activity of morphine. Permeability measurements in Caco-2 cells revealed that **7** has both low A-B permeability ($<1 \times 10^{-6}$ cm/s) and is an efflux substrate (ER >10). When **7** was tested in the presence of P-gp inhibitor *N*-(4-[2-(1,2,3,4-tetrahydro-6,7-dimethoxy-2-isoquinolyl) ethyl]phenyl)-9,10-dihydro-5-methoxy-9-oxo-4-acridine carboxamide (GF120918),⁶¹ the A-B permeability increased to $\sim 4 \times 10^{-6}$ cm/s. In contrast, **8** displayed A-B permeability of 3×10^{-6} cm/s and did not appear to be an efflux substrate. Despite the fact that the two compounds **7** and **8** have identical HBD count and tPSA values and the MW of **8** is higher, the latter has superior permeability and lower efflux. This is likely due to the combination of a more favorable cLogP of 2.6 for **8** relative to 1.2 for **7** and intramolecular masking of the amide NH via H-bonding to the isoquinoline nitrogen atom.⁶² The approach of cloaking of HBD groups via intramolecular H-bonding has proven successful in a number of other scaffolds susceptible to P-gp efflux.

The aspartyl protease β -Amyloid cleaving enzyme-1 (BACE1) is a hotly pursued target in the quest for a disease-modifying therapy for Alzheimer's disease.^{63–65} Reconciling the structural requirements for potency and protease selectivity with the need for low metabolic clearance, adequate passive permeability, and avoidance of P-gp efflux in individual compounds has proven extremely challenging for those that have tackled BACE inhibitor optimization. It is worthwhile contrasting the timeline involved in advancing HIV protease inhibitors from target discovery to drug launch with the time that has elapsed since the first disclosure of BACE as a molecular target. HIV protease was first disclosed in 1988, and remarkably,



Cmpd	hB1 Ki (nM)	P _{app} (x10 ⁻⁶ cm/s) ^a	P-gp ER ^a	MW	cLogP	PSA (Å ²)	HBD
1	0.71	NR	22.6	450	3.6	104.1	2
2	0.93	21	8.6	416	1.0	84.5	2
3	0.4	31	3.2	452	1.6	84.5	2
4	0.57	28	2.3	470	2.6	84.5	2
5	0.13	25	8.6	484	2.3	84.5	2
6	0.44	34	1.9	486	3.1	84.5	2

Figure 5. Attenuation of P-gp efflux in Merck B1 antagonists via amide modification. ^aLLC-PK transfected with human MDR1, NR = not reported.



Cmpd	Mu Ki (nM)	Kappa Ki/ Mu Ki	Delta Ki/ Mu Ki	P-gp ^a ER	P _{app} (x10 ⁻⁶ cm/s) ^a	MW	cLogP	PSA (Å ²)	HBD
NAP(7)	0.37	>150	>700	>10	<1	446	1.2	94.9	3
NAQ(8)	0.55	50	>200	1.3	3	496	2.6	94.9	3

Figure 6. P-gp efflux activity and passive permeability of naltrexamine analogues. ^aMeasured in Caco-2 cells.

within seven short years saquinavir had received FDA approval and was quickly followed by several other entries. BACE was disclosed in 1999 and only recently have first inhibitors begun to enter clinical development, still many years from potential FDA approval. Although there are many factors that distinguish HIV infection from Alzheimer's disease, a major differentiator is the absolute requirement that BACE inhibitors enter the CNS. The requirement for CNS penetration imparts additional confinements around available structural and physicochemical space, reducing the scope to solve potency, selectivity, and pharmacokinetic deficiencies.

Given the similarity between the two aspartyl proteases, it is not surprising that early nonpeptidic BACE inhibitors took advantage of HIV protease inhibitor-inspired statine, hydroxyethylene, and hydroxyethylamine (HEA) transition state (TS) isosteres. However, for a CNS drug target a fundamental issue

resides with the high tPSA and HBD count imparted by each of these TS isostere moieties and their propensity for recognition by P-gp. The FDA-approved HIV protease inhibitors are P-gp substrates.⁶⁶ Whereas P-gp efflux is tolerable for HIV anti-retroviral therapy, it is a major disadvantage for BACE inhibitors targeted for Alzheimer's disease. An example of preserving BACE potency with HEA-based inhibitors while circumventing P-gp efflux has recently been disclosed by researchers at Amgen.^{67,68} Early lead BACE inhibitor **9** (Figure 7) displayed good cell potency (IC₅₀ = 13 nM) and high passive permeability (P_{app} = 20 × 10⁻⁶ cm/s) but failed to reduce CSF Aβ₄₀ levels in rats when dosed up to 30 mg/kg p.o. as a consequence of high P-gp efflux. Compound **9** was a particularly strong substrate for rat P-gp efflux (hP-gp ER = 17 and rP-gp ER = 43). Attempts to remove any of HBDs in the HEA unit met with a steep decline in potency as a result of their key

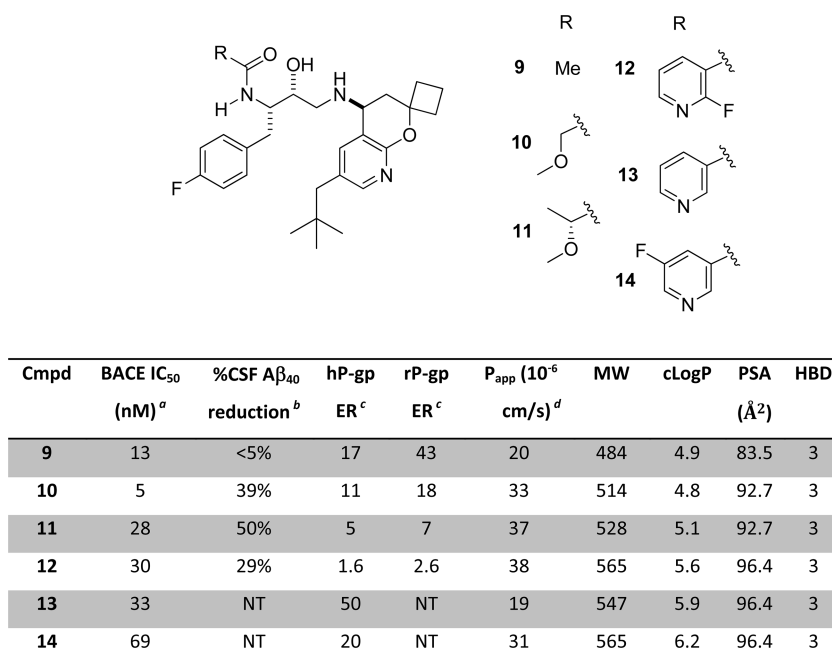
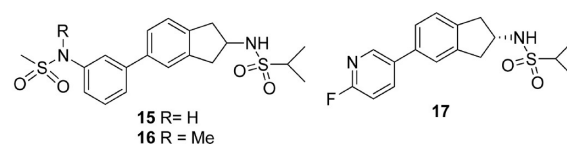


Figure 7. Modulation of P-gp efflux via positioning of hydrogen bond acceptor groups proximal to an amide NH. ^aIn HEK293 cells. ^bIn rat at 30 mg/kg p.o. ^cLLC-PK transfected with human (h) or rat (r) MDRI. ^dParental LLC-PK cells.

roles in a network of hydrogen bond interactions with the two catalytic aspartate residues (Asp228, Asp32) and the flap region of the protein (Gly34) as well as Gly230 and Gln73. An alternative approach was explored involving cloaking the amide NH via intramolecular H-bonding with suitably positioned HBAs. Compounds 10–12 utilizing ether oxygen atoms or a F atom as the HBA for the neighboring amide NH showed progressively improved ERs with moderate effects on cell potency. Gratifyingly, 10, 11, and 12 all reduced CSF Aβ₄₀ levels in rat when testing a screening dose of 30 mg/kg p.o. In support of the hypothesis that intramolecular H-bonding is driving the suppression of P-gp efflux, nicotinamide 13 lacking the F atom present in 12 had a hP-gp ER of 50 and the 5-fluoronicotinamide isomer 14 a hP-gp ER of 20, whereas 2-fluoronicotinamide 12 had a hP-gp ER of 1.6. Although considerably weaker than a classical O...H and N...H H-bonds, existence of intramolecular F...H H-bonding is supported by evidence from NMR and X-ray crystallographic data.^{69,70} Compounds 12 and 13 had equivalent BACE IC₅₀ values. Thus, 12 represents a remarkable compromise, providing satisfactory H-bonding contacts on the biological target of interest but insufficient for P-gp recognition. The calculated tPSA values for 12 and 13 are identical (96.4 Å²); therefore, careful consideration of apparent tPSA and HBA/HBD values should be applied in cases where the potential for intramolecular H-bonding exists.

During assessment of a series of indane-based 2-amino-3-hydroxyl-5-methyl-4-isoxazole-propionic acid (AMPA) receptor positive allosteric modulators, researchers at GlaxoSmithKline, identified early lead compound 15, which possessed promising in vitro potency, efficacy, selectivity, and moderate plasma protein binding (Figure 8).⁷¹ When dosed orally in rats, compound 15 demonstrated acceptable plasma exposure but a poor brain-to-blood ratio (0.1). In vitro testing of 15 using an MDCK cell line expressing human MDRI revealed that, although having good passive permeability, 15 was a substrate for human P-gp (ER = 5.8). The relatively high tPSA imparted by the two sulfonamide moieties suggested these groups as targets for modification to reduce P-gp efflux. Unfortunately,



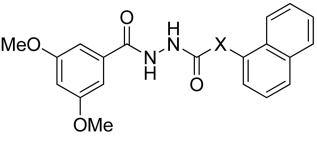
cmpd	hGluA2 pEC ₅₀	P _{app} ^a (10 ⁻⁶ cm/s)	P-gp ER ^b	B/P ratio ^c	MW	cLogP	PSA (Å ²)	HBD
15	6.1	60	5.8	0.1	409	2.7	109.1	2
16	5.9	69	3.2	0.4	423	2.7	100.3	1
17	5.6	68	1.1	2.1	334	2.8	67.4	1

Figure 8. Modulation of P-gp efflux in a series of AMPA potentiators via N-methylation or removal of a secondary sulfonamide. ^aMeasured in MDCK cells expressing human MDRI in the presence of P-gp inhibitor GF120918. ^bEfflux ratio in the absence of GF120918. ^cRat brain–blood AUC_{0-t} ratio.

attempts to replace the sulfonamide at the 2-position of the indane were not tolerated with respect to AMPA receptor potency. N-Methylation of the aryl sulfonamide group (16), however, resulted in minimal change in AMPA potency and efficacy and had the desired effect of lowering the P-gp efflux ratio (ER = 3.2). Consistent with a lower ER, 16 gave an improved brain-to-blood ratio in rats (0.4) but unfortunately had poor systemic exposure. The encouraging CNS penetration properties of 16 suggested that the sulfonamide at the 2-position of the indane could be tolerated for BBB permeability. Further attempts to reduce tPSA then focused on removing the aryl sulfonamide and then restoring potency with alternative groups. After surveying a variety of substituents, it was discovered that replacing the phenyl ring with a 2-fluoropyridyl ring provided adequate AMPA potency. This approach led to compound 17, which had AMPA potency and efficacy approaching that of 15 but with a tPSA of 67.4 Å² compared to 109.1 Å² for 15. Accordingly, in the MDCK-MDRI assay 17

was not a P-gp substrate (ER = 1.1), had good passive permeability, and showed a good brain-to-blood ratio in rats (2.1) with acceptable brain tissue binding as determined by equilibrium dialysis. Compound **17** had low clearance in rats and human liver microsomes and was orally active in a rat novel object recognition behavioral model and dose-dependently attenuated scopolamine-induced amnesic activity in a passive avoidance test. Compound **17** had other favorable pharmacokinetic properties including low PXR activation activity and low potential for drug–drug interactions and was ultimately advanced as a clinical development candidate.

An example of the beneficial effect on P-gp efflux of replacing an NH with a methylene unit has been reported by researchers at Lundbeck investigating agonists of GPR139, a CNS-enriched orphan G-protein coupled receptor.⁷² Compound **18** was identified in a high-throughput screen as an agonist of human GPR139 with an EC₅₀ of 39 nM in a calcium mobilization assay. Although **18** had encouraging GPR139 potency and selectivity against a panel of 90 other targets, it demonstrated a moderate P-gp efflux ratio of 4.1 in an MDR1-MDCK assay, although with good passive permeability. Unfortunately, **18** produced low total brain exposure and a brain/plasma ratio of 0.03 in rats indicating impaired entry into the CNS (Figure 9).



18 X = NH
19 X = CH₂

	18	19
A-B permeability (x10 ⁻⁶ cm/s) ^a	28.8	54
P-gp Efflux ratio ^a	4.1	2.6
GPR139 EC ₅₀ (nM)	39	88
Brain/Plasma ^b	0.03	2.8
Unbound plasma %	1.5	0.4
Unbound brain %	3.5	4.0
Total brain exposure (ng/g)	61	95
Mw	365	364
ClogP	3.5	3.7
PSA (Å ²)	88.7	76.7
HBD	3	2

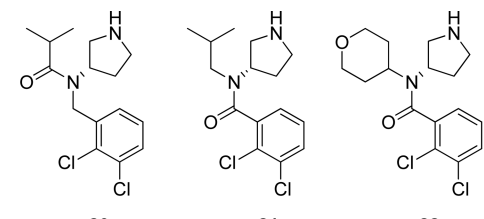
Figure 9. Influence on P-gp efflux and rat brain/plasma partitioning of replacing a single NH group with a methylene unit in a GPR139 agonist. ^aA-B permeability in the MDCK cell assay. ^b50 mg/kg p.o. in rat at 2 h.

Optimization, focused on reducing PSA, led to a set of analogues in which the two hydrazide NH groups were independently replaced with a methylene unit. Unfortunately, these changes resulted in a loss in potency, as did the deletion of the carbonyl group adjacent to the aryl ring. However, replacement of the aryl NH with a methylene unit, resulting in compound **19**, gave only a modest decline in potency (GPR139 EC₅₀ = 88 nM) but provided a sought after decrease in P-gp efflux ratio to 2.6. The resulting exposure in rats revealed an increased brain/plasma ratio of 2.8, although the unbound concentration

in the brain (10.4 nM) at 50 mg/kg p.o. did not exceed the GPR151 EC₅₀ of 88 nM due to low peripheral exposure. The modifications attempted illustrate the challenges of mitigating efflux while maintaining biological target potency and optimizing for good pharmaceuticals and pharmacokinetic properties. However, the replacement of a single NH group with a methylene was sufficient to have a dramatic effect on brain–plasma partitioning.

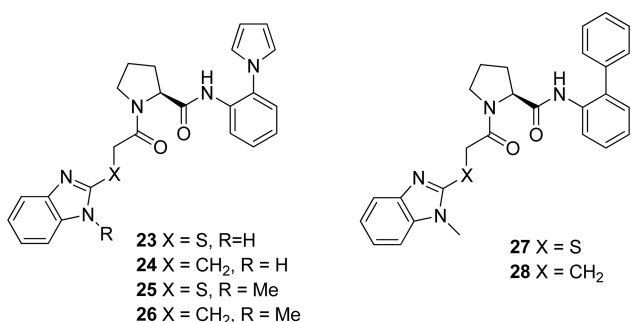
Researchers at Pfizer have developed the dual serotonin and noradrenaline reuptake inhibitor (SNRI) **20** and investigated its efficacy in a dog model for stress urinary incontinence (SUI).⁷³ Surprisingly, **20** failed to produce a statistically significant increase in peak urethral pressure (PUP) in a dose range where the unbound plasma levels of the drug exceeded the in vitro potency of the compound (Figure 10). Assessment of the cerebrospinal fluid (CSF) levels in rats and dogs at steady state revealed that **20** possessed a low free-plasma-to-CSF ratio of 0.1. Despite having properties compatible with good CNS penetration, including a tPSA of 32.3 Å² and MW of 315, **20** showed evidence of P-gp efflux (ER = 4.3) in an mdr1-MDCK assay. Given the already low tPSA of **20** and the requirement for the presence of the basic pyrrolidine N for good SNRI potency, a strategy was formulated to reduce efflux by altering the H-bonding properties of the compound, specifically via transposing the amide carbonyl with the benzylic methylene group. Remarkably, the resulting amide isomer **21** displayed an ER of 2.7 in the mdr1-MDCK assay while maintaining excellent SNRI potency. Interestingly, the more polar 4-tetrahydropyranyl analogue **22** produced an ER of 20 in the mdr1-MDCK assay. When **21** was assessed in the dog SUI model, it elicited a dose-dependent increase in PUP superior to that observed with SNRI duloxetine. Compound **21** (PF-184,298) possessed a pharmacokinetic and preclinical toxicology profile sufficient to support its progression into human clinical studies. This example represents an elegant and effective use of the repositioning of hydrogen bonding functionality to diminish P-gp recognition. This approach is particularly valuable for low PSA compounds where the alternative of navigating to even lower PSA to evade efflux would drive further toward the physicochemical space associated with increased odds of off-target activity and higher probability of safety failure.⁷⁴ As will be discussed in other P-gp mitigation cases, the presence of a strongly basic amine can often predispose a compound series to P-gp recognition.

5.2. Heterocyclic NH Groups. Orexins A and B are neuropeptides that exert activity on two receptors: orexin 1/orexin 2 (OX₁/OX₂) expressed in the CNS. Orexin deficiency results in narcolepsy, and brain penetrant orexin receptor antagonists have garnered significant interest for treating sleep disorders. Researchers at Merck have recently described the discovery and optimization of a series of dual OX₁/OX₂ receptor antagonists (Figure 11).⁷⁵ The proline derived bisamide **23** was identified as a screen hit with promising potency at both OX₁ (K_i = 28nM) and OX₂ (K_i = 1nM) receptors. During the initial optimization process, it became evident that the early lead compounds **23** and **24** were substrates for P-gp efflux. In an attempt to lower the PSA and HBD count, the N-Me imidazole analogues **25** and **26** were prepared. Addition of the N-Me group not only had the desired effect of rendering **25** and **26** devoid of P-gp efflux but also had the additional benefit of improving potency at both OX₁ (K_i = 9 nM and 46 nM, respectively) and OX₂ (K_i = 0.3 nM and 2 nM, respectively) receptors. Independent, modification of the 2-pyrrolyl to a



cmpd	5-HT Ki (nM)	NA Ki (nM)	DA Ki (nM)	P-gp ^a ER	MW	cLogP	cLogD (pH 7.4)	pKa ^b	PSA (Å ²)	HBD
20	9	52	640	4.3	315	3.3	0.8	9.5	32.3	1
21	6	21	544	2.7	315	3.6	1.2	9.3	32.3	1
22	6	10	945	20	343	1.8	0.04	9.3	41.6	1

Figure 10. Modulation of P-gp efflux via amide transposition in a series of dual serotonin and noradrenaline reuptake inhibitors. ^aMeasured in MDCK cells expressing mdr1. ^bCalculated.



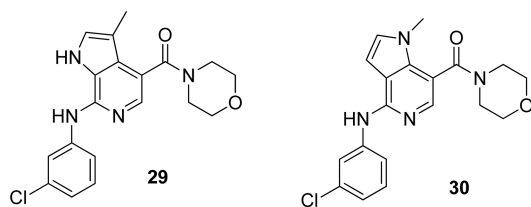
	23	24	25	26	27	28
P-gp Efflux ratio	6.8	13	2	2	1.4	2
hOX₁ Ki (nM)	28	130	9	49	3	15
hOX₂ Ki (nM)	1	11	0.3	2	0.2	0.8
Brain/plasma/CSF (nM)^a	NR	NR	NR	NR	2370/3500/43	13007/25705/860
Mw	446	427	460	442	471	453
ClogP	4.0	3.1	4.3	3.6	4.4	3.6
PSA (Å²)	107.8	82.5	96.9	71.6	92.5	67.2
HBD	2	2	1	1	1	1

Figure 11. Mitigation of P-gp efflux in a series of orexin antagonists via N-methylation of a benzimidazole. ^a100 mg/kg ip 30 mins in rat; NR = not reported.

phenyl was shown to further enhance potency, and when this change was combined with the *N*-methylbenzimidazole finding, the resulting analogues **27** and **28** both displayed further improved OX₁ and OX₂ potency and maintained an absence of P-gp efflux. Thirty minutes after ip dosing in rats at 100 mg/kg, the CSF levels of **27** exceeded its K_i at OX₁ and OX₂ by 14- and 215-fold, respectively, and those of **28** exceeded its K_i at OX₁ and OX₂ by 57- and 1075-fold, respectively. This example further demonstrates the significant influence of NH groups on P-gp efflux.

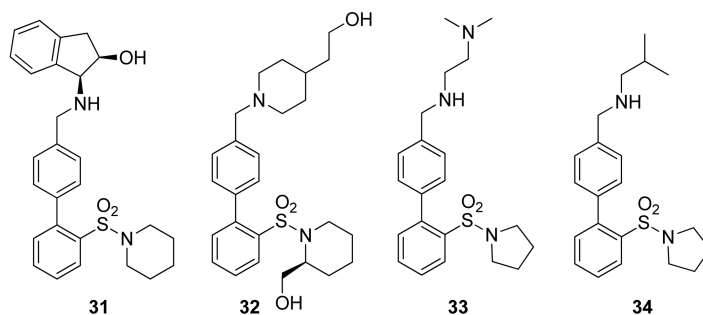
A second example of substantial suppression of P-gp efflux involving removal of the heterocyclic NH group, this time combined with an attenuation of basicity, is illustrated in Figure 12. During the optimization of cannabinoid CB₂ agonists for pain, 6-azaindole **29** was identified as a lead compound with favorable CB₂ agonist efficacy and potency (CB₂ EC₅₀ = 11 nM) and good selectivity over CB₁ receptor agonism (CB₁ EC₅₀ = 10000 nM).⁷⁶ Although **29** had promising in vitro clearance in rat and human

liver microsomes and a favorable CYP450 inhibition profile, in a rat joint model of chronic pain that is sensitive to COX2 inhibitors, **29** had no significant analgesic effect when dosed orally at 1, 3, or 10 mg/kg bid for 5 days. In contrast, rofecoxib gave a full reversal of hyperalgesia at an oral dose of 5 mg/kg bid. The brain/blood ratio of **29** in rat was found to be low (<0.05), and it was reasoned that this may be responsible for the absence of efficacy in the chronic pain model. Compound **29** was found to possess a high P-gp efflux ratio (ER = 74), and attempts were initiated to reduce the hydrogen bond donor count to suppress efflux. Unfortunately, direct N-methylation of the azaindole NH resulted in a large decrease in potency (CB₂ EC₅₀ = 654 nM). As an alternative, the isomeric 5-azaindole analogue **30** (GSK554418A) was prepared, and fortunately, this compound retained good CB₂ activity (CB₂ EC₅₀ = 8 nM) and demonstrated dramatic improvement in P-gp efflux ratio (ER = 2.9) and a high blood/brain ratio of 1.04 in rat after iv administration over 12 h. The contrasting P-gp efflux ratios of **29**



cmpd	CB2 EC ₅₀ (nM)	P-gp ^a ER	Rat B/P ratio	MW	cLogP	cLogD (pH 7.4)	pKa ^b	PSA (Å ²)	HBD
29	11	74	<0.05	371	2.3	1.4	8.3	70.3	2
30	8	2.9	1.04	371	2.2	2.2	6.3	59.4	1

Figure 12. Dramatic shift in P-gp efflux during the optimization of azaindole CB2 agonists. ^aAssay used for P-gp determination was not described. B/P = brain/plasma ratio after iv dosing. ^bCalculated for the most basic center.



cmpd	Kappa K _i (nM)	Mu K _i (nM)	P-gp ER	HLM (μl/min/mg)	MW	cLogP	cLogD (pH 7.4)	pKa ^a	PSA (Å ²)	HBD
31	9	21	2.56	>300	463	4.6	4.1	7.8	78.0	2
32	1.1	32	14	163	473	2.8	1.5	8.5	89.5	2
33	5.8	101	4.68	20	388	3.3	1.1	9.3	61.0	1
34	3	64	1.96	27.6	373	4.3	2.3	9.4	57.8	1

Figure 13. Attenuation of P-gp efflux in a series of κ -opioid receptor antagonists. ^aCalculated for the most basic center.

and **30** are quite remarkable given their relatively minor structural and physicochemical differences (1 HBD and 10.9 Å² of tPSA). However, the 5-azaindole **30** also has a significantly lower calculated pK_a of 6.3 compared to 8.3 for **29**. The weaker basicity of **30** may contribute to the dramatically lower efflux ratio observed with the compound. In the chronic joint pain model, **30** showed full reversal of hypersensitivity when dosed twice daily for 5 days at an oral dose of 10 mg/kg, with efficacy equivalent to that of an oral dose of rofecoxib, and a minimally effective dose of 3 mg/kg.

5.3. Basic Amines. Seeking selective κ -opioid receptor antagonists as a potential novel approach to treating depression, researchers at Pfizer identified a biphenylamine hit **31** (Figure 13) from a high throughput screen.⁷⁷ Profiling of **31** revealed it as a moderate substrate for P-gp (ER = 2.56), in addition to having high in human microsomal clearance and insufficient selectivity over the μ -opioid receptor. Initial optimization focused on improving ligand efficiency and lipophilicity—ligand efficiency within the property guidelines of $M_w < 425$, <2 HBD and clogD < 3. Compounds **32**, **33**, and **34** all possessed μ -receptor K_i < 10 nM and met the target of >20 \times selectivity over the κ -receptor along with improved human microsomal stability. Perhaps not surprisingly, **32** possessing 2 HBD and 89.5 Å² of tPSA displayed strong P-gp efflux properties (ER = 14.0).

The contrast between **33** and **34** reveals an interesting influence of removing one of the two basic N atoms in **33** on P-gp efflux. The loss of one N modestly reduces tPSA by 3.2 Å² but results in **34** giving an ER = 1.96 compared an ER = 4.68 observed with **33**. The predictive value of in vitro P-gp efflux was borne out in vivo and provides a fascinating comparison between the strong, moderate, and low P-gp efflux properties of **32**, **33**, and **34**, respectively. An in vivo exposure–response relationship for κ -opioid antagonism was established in rat using a tail flick analgesia model by measuring the reversal of the nociception induced by the selective κ -opioid agonist (2-(3,4-dichlorophenyl)-N-methyl-N-[(1R,2R)-2-pyrrolidin-1-ylcyclohexyl]acetamide), U50488H.⁷⁸ The free plasma levels of the test compound after subcutaneous dosing and normalization for κ K_i potency (free plasma/ κ -binding K_i) were plotted against the percent reversal of U50488H-induced nociception. For maximal nociception reversal, the free plasma/ κ K_i values of **34**, **33**, and **32**, were ~3, ~30, and >100, respectively. The increasing asymmetry between free plasma levels and in vivo CNS effect are presumably a reflection of the increasing P-gp efflux of the three compounds. Additional pharmacokinetic profiling of compound **34** (PF-4455242) revealed a good correlation among rat CSF, free plasma, and unbound brain exposure. The compound has been advanced into a phase I human clinical trial.

compd	B1 K_i (nM)	P_{app}^a ($\times 10^{-6}$ cm/s)	P-gp ^o ER	MW	cLogP	cLogD (pH 7.4)	pKa ^b	PSA (\AA^2)	HBD
35	45	27	2.5	394	4.2	4.1	-	100.7	2
36	0.25	34	14	521	5.9	3.9	9.4	116.0	3
37	2.1	21	4.8	523	4.2	4.0	7.2	125.2	3
38	0.7	26	2.3	481	4.9	4.8	-	119.2	2
39	2.6	31	2.6	482	3.6	3.6	2.6	132.1	2
40	0.2	26	3.1	500	3.8	3.5	0.2	132.1	2

Figure 14. Reduction in P-gp efflux in a B1 antagonist series in response to attenuation or removal of a basic amine. ^aLLC-PK cells expressing human MDRI. ^bCalculated for the most basic center.

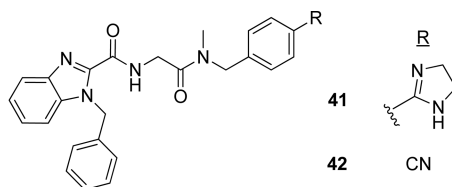
A second example illustrating the influence of basic functionality on P-gp efflux is shown in Figure 14. Researchers at Merck identified the benzophenone screen hit **35** as a bradykinin B1 antagonist with promising potency (human B1 $K_i = 45$ nM), good passive permeability ($P_{app} = 27 \times 10^{-6}$ cm/s), and with an absence of significant P-gp efflux in vitro (ER = 2.5).⁷⁹ However, **35** behaved as a PXR activator in vitro and was rapidly metabolized in microsomal incubations. During efforts to increase potency and metabolic stability, appending a basic amine group in the side chain was explored, resulting in analogue **36**, which possessed a B1 $K_i = 0.25$ nM, in addition to improved PXR and metabolic stability properties. However, the modifications leading to **36** significantly increased MW, tPSA, and cLogP, and added an additional HBD. In contrast to **35**, compound **36** behaved as a strong P-gp substrate with an ER = 14. To reduce P-gp and hERG activity, attention focused on attenuating the basicity of the amino group in **36** (calculated $pK_a = 9.4$). This approach resulted in morpholine analogue **37** (calculated $pK_a = 7.2$), which showed an improved P-gp profile (ER = 4.8). Replacement of the basic moiety altogether with a tetrahydrofuran and switching the urea linker for a carbamate in the form of **38** had a further beneficial effect on reducing efflux (ER = 2.3) without any significant erosion of B1 affinity (B1 $K_i = 0.7$ nM). Further refinements to bolster metabolic stability involved changing the phenyl ring for 2-pyridyl (**39**) and 5-fluoro-2-pyridyl (**40**) groups, which had minimal effects on P-gp efflux ratios. Consistent with its high passive permeability and lack of P-gp efflux, after iv infusion, **38** showed dose-dependent receptor occupancy in the brain and spinal cord of transgenic rats overexpressing the human B1 receptor. In this series, the detrimental influence of a basic center and a third HBD is apparent in the high ER ratios observed with compounds **36** and **37**. It is remarkable that compounds **38**, **39**, and **40** all have low efflux ratios despite their high tPSA (119.2 \AA^2 to 132.1 \AA^2) and the presence of 2 HBD groups. Intramolecular

H-bonding between the sulfonamide NH and the ketone carbonyl is likely serving to mask the availability of these groups to interact with P-gp.

As exemplified by the case described above, reducing the basicity of amino groups is a proven strategy for reducing P-gp efflux. In a related case in the oncology field, researchers at Merck have recently disclosed a creative example of optimization away from P-gp efflux in a series of Kinesin spindle protein (KSP) inhibitors via modulating the basicity of the amino group by β -fluorination, resulting in compounds with greatly improved efficacy in a Pgp-overexpressing cell line.⁸⁰

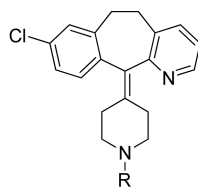
Rationally designed using a scaffold hopping strategy, early Neurogen B1 antagonist lead compound **41** displayed encouraging potency (cynomologous macaque B1 $IC_{50} = 5$ nM) (Figure 15).⁸¹ Compound **41**, however, had low passive permeability (1×10^{-6} cm/s) and was determined to be a strong P-gp substrate (ER = 23) in an MDRI-MDCK assay. This finding was confirmed by testing the permeability of the compound in the presence of the P-gp inhibitor cyclosporine (25 nM), which resulted in the passive permeability of **41** increasing to 11×10^{-6} cm/s and the ER decreasing to 1.5. To probe the role of the basic imidazoline moiety on permeability, this group was replaced with a nitrile giving compound **42**. While **42** possessed tPSA virtually identical to that of **41**, it had one fewer HBD and lacked the basic center of **41**, resulting in **42** having substantially improved passive permeability (7×10^{-6} cm/s) and a significantly lower ER (ER = 3). Extensive efforts to replace the imidazoline in **41** unfortunately only led to compounds with greatly diminished B1 potency, illustrating the longstanding challenge of balancing potency and permeability (and clearance) in the B1 antagonist field.

A number of Histamine H1 receptor antagonists have been developed as drugs to treat allergic disorders including rhinitis and asthma. The so-called second generation H1-antagonists cetirizine, loratadine, fexofenadine, and desloratadine produce



Cmpd	cB1 ^a IC ₅₀ (nM)	P-gp ER ^b	P-gp ER with CS ^c	P _{app} ^b (10 ⁻⁶ cm/s)	P _{app} with CS (10 ⁻⁶ cm/s)	MW	cLogP	cLogD (pH 7.4)	pKa ^d	PSA (Å ²)	HBD
41	5	23	1.5	1	11	481	4.9	0.4	9.9	89.4	2
42	>5000	3	NT	7	NT	437	3.8	3.4	3.3	88.8	1

Figure 15. Dramatic effect on P-gp efflux effect and passive permeability of switching an imidazoline to a nitrile in a B1 antagonist series. ^aCynomologous B1. ^bMDCK cells transfected with human MDR1. ^cCS = cyclosporine (25 μM). ^dCalculated for the most basic center.



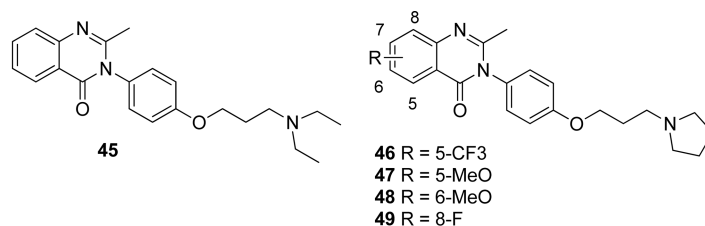
43 Loratadine R = CO₂Et
44 Desloratidine R = H

Cmpd	P-gp ER ^a	B/P in P-gp KO vs WT ^b	MW	cLogP	cLogD (pH 7.4)	pKa ^c	PSA (Å ²)	HBD
Loratadine (43)	1.9	2.0	382	5.9	5.9	4.3	42.4	0
Desloratidine (44)	9.1	>14	310	6.8	4.1	10.3	24.9	1

Figure 16. Increased P-gp efflux of desloratidine, the basic amine containing a metabolite of loratadine, translates into lower CNS exposure and reduced CNS side effects. ^aMDCK cells transfected with human MDR1. ^bBrain-to-plasma AUC ratios in *mdr1a*(^{-/-}) versus *mdr1a*(^{+/+}) mice after 5 mg/kg iv dose. ^cCalculated for the most basic center.

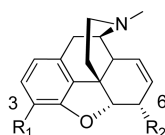
minimal somnolence or other CNS side effects at their therapeutic exposures. A retrospective analysis of the CNS penetration characteristics of these four drugs in wild type versus *mdr1a*(^{-/-}) knockout mice indicates that these compounds are all in fact substrates for P-gp.⁸² In contrast, the first generation H1-antagonists diphenhydramine, triprolidine, and hydroxyzine, which frequently produce somnolence or other CNS adverse effects, have equivalent brain-to-plasma ratios in wild type and *mdr1a*(^{-/-}) mice. Thus, the benefit of P-gp efflux in reducing CNS side effects is apparent in the second generation H1-antagonists. However, it should be noted that the introduction of P-gp efflux was not by conscious design but rather by “natural selection” and was discovered retrospectively.⁸³ For example, desloratidine (44), an active circulating metabolite, and its parent loratadine (43), are both substrates of P-gp although the extent of efflux is much more pronounced in the former (Figure 16). The P-gp efflux ratio in MDR1-MDCK cells for 44 is 9.1 versus 1.9 for 43, and this efflux ratio difference is readily apparent in vivo. The brain-to-plasma area under the curve (AUC) ratio for loratadine is 2-fold versus >14-fold for desloratidine when exposures are compared in *mdr1a*(^{-/-}) mice with those in *mdr1a*(^{+/+}) mice. Thus, despite adding additional PSA and molecular weight, the amine-masking carbamate group in loratadine translates into a compound having a much lower ER when compared to that of its smaller and less polar but more basic metabolite desloratidine.

Antagonists and inverse agonists of the histamine H3 receptor have been of interest for CNS disorders including schizophrenia, cognitive dysfunction, and excessive daytime sleepiness. Researchers at Merck-Banyu have disclosed an interesting example of species dependent P-gp efflux encountered with a series of quinazolinone H3 inverse agonists (Figure 17).⁸⁴ High throughput screen hit 45 provided a useful starting point (H3 IC₅₀ = 33 nM), optimization of which initially focused on increasing H3 potency while minimizing hERG affinity. SAR in the quinazolinone ring resulted in analogues 46, 47, 48, and 49 with sufficient potency and selectivity over hERG binding to justify broader profiling. All four compounds 46–49 were substrates for mouse *mdr1a* when tested in LLC-PK cells expressing mouse *mdr1a* with ER ratios ranging from 13 to 5.1. Additionally, compounds 47 and 49 were also substrates for human P-gp with ERs of 11.4 and 3.9, respectively. Compounds 46 and 48, however, with ERs of 2.4 and 3.0, were classified as nonsubstrates for human P-gp. Compound 46 was also a substrate for rat P-gp (ER = 7.3) when tested against rat *mdr1a* expressed in LLC-PK cells. Compound 46 had favorable in vitro and in vivo pharmacokinetic properties and was tested for brain exposure and H3 receptor occupancy in wild type (*mdr1a*(^{+/+})) and P-gp-deficient (*mdr1a*(^{-/-})) CF-1 mice. At 10 mg/kg p.o. in *mdr1a*(^{-/-}) mice, the brain/plasma ratio of 46 was 14 versus a brain/plasma of 0.8 in *mdr1a*(^{+/+}) mice. The plasma levels to achieve 90% H3 receptor occupancy in *mdr1a*(^{-/-}) mice were 1.17 nM versus 40 nM in *mdr1a*(^{+/+})



Cmpd	H3 IC ₅₀ (nM) ^a	hP-gp ER ^c	mP-gp ER ^c	rP-gp ER ^c	MW	cLogP	cLogD (pH 7.4)	pKa ^d	PSA (Å ²)	HBD
46	1.7	2.4	13	7.3	431	3.4	0.8	10.2	45.1	0
47	1.3	11.4	7.9	NR	393	2.8	0.1	10.2	54.4	0
48	1.1	3.0	5.1	NR	393	2.8	0.1	10.2	54.4	0
49	1.5	3.9	10	NR	381	2.9	0.3	10.2	45.1	0

Figure 17. H3 antagonists with differential human and mouse P-gp efflux properties. ^aLLC-PK transfected with human MDR1, mouse *mdr1a*, or rat *mdr1a*; NR = not reported.

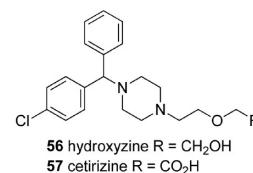


cmpd	R1	R2	μ Ki (nM) ^a	δ/μ	κ/μ	P-gp ^b substrate	MW	cLogP	cLogD (7.4)	pKa ^c	PSA (Å ²)	HBD
50	OH	OH	1.7	61	38	yes	285	0.4	-0.4	8.2	52.9	2
51	OMe	OH	727	72	35	yes	299	1.2	0.3	8.2	41.9	1
52	OH	OMe	1.1	60	21	yes	299	1.0	0.3	8.2	41.9	1
53	OMe	OMe	1910	2	3	No	313	1.7	0.9	8.1	30.9	0
54	OH	H	2.9	4	16	No	269	1.9	0.8	8.6	32.7	1
55	OMe	H	305	15	10	No	283	2.7	1.5	8.6	21.7	0

Figure 18. P-gp efflux properties of morphine analogues. ^aDetermined using [³H]diprenorphine binding. ^bP-gp Glo ATP assay with 200 μM test compound. ^cCalculated for the most basic center.

mice. However, the brain levels to achieve 90% H3 receptor were virtually identical in in *mdr1a*^(-/-) and *mdr1a*^(+/+) mice. The in vivo impact of P-gp efflux on peripheral drug load and dose to achieve CNS target occupancy is elegantly illustrated in this set of experiments. In addition, the high efflux ratios of 46–49, in spite of their generally low polar surface area and an absence of a HBD, are noteworthy. As has been observed in other examples, the presence of a basic center can serve to lower the tPSA threshold at which P-gp efflux becomes problematic. The lack of concordance between mouse and human P-gp efflux ratios should also caution against relying solely on human MDR1 for efflux assessment. The shifts in P-gp ERs in response to subtle substituent changes in the quinazoline ring provide some reason for optimism that the latitude to modulate P-gp recognition exists within narrow structural space.

5.4. Alcohols and Phenols. As mentioned previously, morphine (50) is a substrate for P-gp, and there is growing evidence that the development of tolerance to opioid analgesics involves a component related to the up-regulation of expression of P-gp at the BBB.⁸⁵ In order to further understand the mechanisms of opioid resistance and develop potential therapeutics with lower potential for the development of tolerance, Coop and co-workers have investigated structural modifications of morphine intended to diminish P-gp efflux while maintaining μ-opioid receptor potency and selectivity (Figure 18).⁸⁶ The

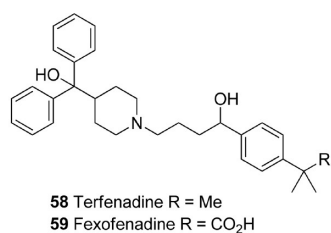


Cmpd	P-gp ER ^a	B/P in P-gp KO vs WT ^b	MW	cLogP	cLogD (pH 7.4)	PSA (Å ²)	HBD
Hydroxyzine (56)	NR	1.2	375	2.0	2.0	35.9	1
Cetirizine (57)	5.8	4.4	389	2.2	-0.9	53.0	1

Figure 19. Increased in vivo P-gp efflux of the carboxylic acid-containing H1 antagonist cetirizine relative to the parent alcohol hydroxyzine. ^aMDCK cells transfected with human MDR1. ^bBrain-to-plasma AUC ratios in *mdr1a*^(-/-) vs *mdr1a*^(+/+) mice after 5 mg/kg iv dose; NR = not reported.

authors used a P-gp Glo assay that uses firefly luciferase to determine the consumption of ATP by P-gp. A decrease in luminescence signifies a drop in ATP levels due to an increase in P-gp activity. Morphine and both analogues 51 and 52, wherein either the 3- or 6-hydroxy group is capped with a methyl group, all behaved as P-gp substrates. The 3-methoxy analogue 51 was significantly less potent ($K_i = 727$ nM) at the

μ -receptor than morphine ($\mu K_i = 1.1\text{nM}$) whereas the 6-methoxy analogue **52** retained μ -potency ($K_i = 1.1\text{ nM}$). Capping both OH groups with methyls rendered the resulting compound **53**, a nonsubstrate for P-gp, but resulted in a major loss in μ -potency, as might have been expected ($K_i = 1910\text{ nM}$). Removal of the 6-OH group as represented in compound **54** produced a desired compromise between potency ($\mu K_i = 2.9\text{nM}$) and lack of P-gp efflux, although with less selectivity over the δ - and κ -subtypes relative to that achieved with morphine. Again, capping the 3-hydroxy group (**55**) resulted in a significant erosion of potency ($\mu K_i = 305\text{ nM}$) but preserved the absence of P-gp efflux observed with **54**. Compound **54** proved to be approximately 10 times more potent than morphine based on dose ($\text{ED}_{50} = 0.2$ vs 1.92 mg/kg sc) in a mouse tail flick assay. It is noteworthy that very



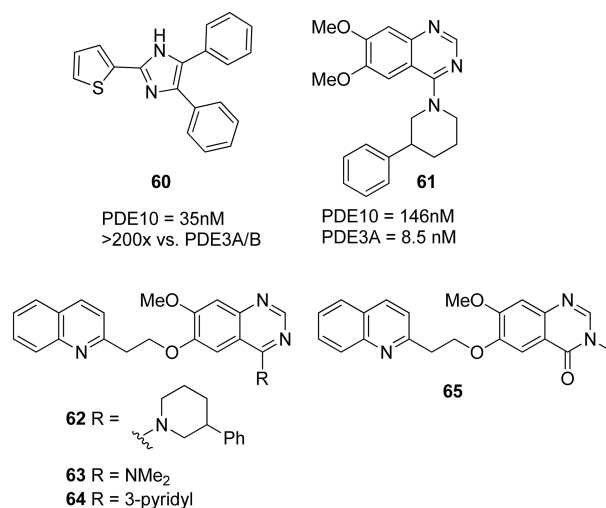
Cmpd	P-gp ER ^a	P _{app} (x10 ⁶ cm/s) ^a	MW	cLogP	cLogD (pH 7.4)	PSA (Å ²)	HBD
Terfenadine(58)	2.9	28.5	472	6.5	4.5	43.7	2
Fexofenadine(59)	6.8	6.6	502	4.8	2.3	81.0	3

Figure 20. Increased P-gp efflux and lower passive permeability of the carboxylic acid-containing H1 antagonist fexofenadine relative to the parent terfenadine. ^aMDCK cells transfected with human MDR1.

low tPSA is required ($<33\text{ Å}^2$) in the morphine scaffold to secure evasion of P-gp efflux. As has been observed in other scaffolds (e.g., H3 antagonists and SNRIs), the presence of a basic center may again lower the threshold for tPSA tolerance before P-gp recognition is triggered.

5.5. Carboxylic Acids. A second example of an active metabolite that resulted in a marketed H1 antagonist drug with reduced CNS exposure is that of cetirizine (**57**). The P-gp efflux ratio in MDR1-MDCK cells for cetirizine is 5.8. The brain-to-plasma area under the curve (AUC) ratio in *mdr1a*^(-/-) mice compared with that of *mdr1a*^(+/+) mice for **57** is 4.4-fold, whereas its precursor hydroxyzine (**56**) has equivalent exposure ratios in wild-type and P-gp knockout mice (Figure 19).⁷⁹ Thus, the structural difference of a hydroxyl group versus a carboxylic acid has a significant influence on P-gp efflux in vivo. A similar situation is encountered when comparing H1 antagonist terfenadine (**58**) with its acid bearing metabolite fexofenadine (**59**) (Figure 20). Compound **58** has high passive permeability ($P_{\text{app}} = 28.5 \times 10^{-6}\text{ cm/s}$), rapidly penetrates the CNS, and does not show markedly different brain uptake in wild type versus *mdr1a*^(-/-) mice.^{87,88} Compound **59**, however, has low passive permeability ($P_{\text{app}} = 6.6 \times 10^{-6}\text{ cm/s}$), displays slow brain uptake, and has steady state brain-to-plasma ratios of 0.005 in *mdr1a*^(+/+) mice and 0.27 in *mdr1a*^(-/-) mice giving an in vivo efflux ratio of ~ 50 . Thus, the presence of the carboxylic acid moiety in **59** simultaneously reduces passive permeability relative to that of **58** and acts as a recognition element for P-gp efflux. On the basis of its improved safety profile, **59** has superseded **58**, which was withdrawn from the US market in 1997 due to issues with QT interval prolongation.

5.6. Increasing Ligand Efficiency (LE). PDE10A is a dual cGMP and cAMP phosphodiesterase that is highly enriched in



cmpd	PDE10A IC ₅₀ (nM)	Papp (x10 ⁶ cm/s)	P-gp ER	MW	cLogP	cLogD (pH 7.4)	pKa ^a	PSA (Å ²)	HBD
62	12	NR	>10	491	5.4	3.3	9.8	60.4	0
63	14	19	0.9	374	3.3	2.8	7.7	60.4	0
64	5	0.4	1.5	408	2.9	2.9	4.7	70.0	0
65	12	18	0.6	361	2.2	2.2	4.9	64.0	0

Figure 21. Truncated PDE10A inhibitors with improved P-gp efflux properties. NR = not reported. ^aCalculated for the most basic center.

medium spiny neurons in the striatum and has been of significant contemporary interest as a drug target for schizophrenia. Researchers at Pfizer identified a quinazoline-based series that possessed good PDE10A inhibitor potency but insufficient selectivity over PDE3A and PDE3B, of concern due to potential cardiotoxicity.⁸⁹ Using information from a cocrystal structure of PDE10A with imidazole hit **60** (Figure 21), which possessed improved PDE3A and PDE3B selectivity, and comparing it against a cocrystal structure of the quinazoline-based scaffold (e.g., **61**) provided a rational approach to improving PDE10A isoform selectivity. The thiophene ring present on imidazole hit **60** exploits a hydrophobic pocket that distinguishes PDE10 from the other 10 members of the PDE family. It was reasoned that this “selectivity pocket” could potentially be accessed via extension from the 6-position on quinazoline ring. This hypothesis resulted in the synthesis of a library of compounds including \pm **62**. Although \pm **62** achieved the goal of securing both good PDE10A potency ($IC_{50} = 12$ nM) and $>100\times$ selectivity over PDE3A, \pm **62** was a P-gp efflux substrate ($ER > 10$) and had poor human microsomal stability. Optimization efforts focused on reducing molecular weight and lipophilicity and improving ligand efficiency to address these issues. Analysis of the ligand efficiency (LE) contributed by the 3-phenylpiperidine fragment relative to the remainder of the molecule in **62** suggested that the 3-phenylpiperidine diminished overall LE and that therefore this group should be prioritized for optimization. Truncated analogues **63**, **64**, and **65** provided equivalent or better PDE10A potency relative to \pm **62** but with weaker basicities, improved cLogP values, and higher LE as a consequence of the smaller structures. The smaller and less basic analogues **63** and **65** also had substantially improved efflux properties with both compounds showing high A-B permeability and no evidence of P-gp efflux. Interestingly, whereas **63** and **65** possessed high passive permeability, the 3-pyridyl analogue **64** had low A-B permeability. Although **64** appeared not to be a substrate for P-gp efflux, it should be noted that efflux ratio values become increasingly unreliable as permeability values decline. Compounds **63**, **64**, and **65** all increased brain cGMP levels in mouse after sc dosing. Despite its low permeability, **64** had better human microsomal stability relative to those of **63** and **65** and was tested in conditioned avoidance responding, showing activity in wild-type ($ED_{50} = 3.2$ mg/kg sc) but not PDE10A knockout mice.

6. CONCLUSIONS

The presence of P-gp efflux in compounds intended for treating CNS disorders increases the probability of failure in the drug discovery process. From a safety and pharmacokinetic standpoint, active efflux at the BBB increases the peripheral drug load necessary for CNS target engagement, introduces the potential for drug–drug interactions and higher intersubject variability and amplifies the uncertainty in projecting human pharmacokinetics and doses. However, for peripherally targeted therapeutics, P-gp efflux has been shown to endow compounds with reduced CNS side effects.

The reader will note the preponderance of cases described in this review where the biological target has an amino acid or peptide as an endogenous ligand or substrate. The bradykinin, orexin, and opioid peptide GPCRs, the receptors for histamine and AMPA, and the aspartyl protease β -secretase all fall into this category. It is unlikely that pure coincidence has led in the majority of published cases of P-gp efflux mitigation being

centered on peptide recognizing targets. As can be gleaned from the examples described, the structural elements that predispose compounds to P-gp efflux frequently overlap with those that favor affinity for such targets. In contrast, the repertoire of approved CNS drugs is dominated by compounds that directly engage biogenic amine receptors or indirectly modulate their activity via inhibition of neurotransmitter metabolism or uptake. This circumstance owes much to the capacity for achieving high affinity at such targets with low molecular weight compounds (high ligand efficiency) that have relatively low tPSA and aided by a traditionally low stringency for biological target selectivity. The industry shift from phenotypic screening and polypharmacology to single-targeted therapeutics has been particularly detrimental to CNS drug discovery success rates.⁹⁰ The often high conservation of orthosteric binding sites among biogenic amine GPCR family members has required subtype selective ligands for even these “low hanging fruit” targets to rely on additional interactions in nonconserved binding regions, thus driving up molecular weight. The surge of interest in allosteric receptor modulators is partly in response to the challenge of attaining selectivity within the confines of CNS-accessible chemical space.⁹¹ The origins of low success rates at each stage of drug discovery are multifactorial, but the limited structural space available to the medicinal chemist intent on achieving selective target engagement in the brain is a major contributing element to the high attrition in CNS programs.

Functional groups that particularly favor P-gp recognition are typically those adorned with HBDs and include primary and secondary amides, ureas, sulfonamides, alcohols, phenols, carboxylic acids, and N-heterocycles bearing uncapped NH groups. In cases where removing the NH or OH via the direct addition of an alkyl or aryl group is not tolerated, then more creative approaches can be explored. Cloaking HBD groups in compounds via the appropriate positioning of a neighboring HBA group has been shown in several cases to offer a compromise between satisfying the H-bond donor contacts necessary for biological target potency but not sufficient to engage P-gp efflux. Other successful approaches at reducing HBD count and tPSA have deployed isosteres as surrogates for P-gp efflux triggering groups. General guidelines for minimizing P-gp recognition include maximizing ligand efficiency, keeping the HBD count below 2 and the tPSA below 90 \AA^2 and preferably below 70 \AA^2 . As exemplified by morphine and H3 antagonists, it appears that the presence of a basic amino group can often further lower the threshold for tPSA tolerance before P-gp efflux is triggered in a compound series. In these types of cases, if lowering of PSA is incompatible with retaining biological activity, modulating the amine basicity or repositioning polar functionality has proven effective. Simple physicochemical guidelines and computational models can be helpful in altering the probability of encountering P-gp efflux; however, it is abundantly evident that compounds with identical physicochemical properties can have vastly different efflux properties. As with any small molecule–protein interaction, the composition and presentation of functionality on a molecule play a critical role in the recognition process. However, unlike the typical small molecule–drug target interaction, P-gp is a highly permissive protein recognizing a wide diversity of substrates. Other antitargets such as hERG and PXR, although not as permissive as P-gp, present similar challenges. The relatively poorly defined molecular interactions that confer P-gp efflux emphasize the value of empirical data to establish structure–efflux relationships early in compound optimization. Improved

in vitro P-gp assays, particularly the MDR1-MDCK and LLC-PK cell-based assays, offer good in vivo predictive value and are a major asset in this regard. The practitioner should be aware of the potential for divergence between rodent and human P-gp susceptibility of compounds and the potential for alterations in BBB efflux and permeability in animal models. Structural modifications that alter P-gp recognition properties ultimately need to be accomplished within the broader context of optimization for safety and efficacy including potency, selectivity, and pharmacokinetic properties.

AUTHOR INFORMATION

Corresponding Author

†Phone: (561) 210-7705. E-mail: stephen.hitchcock@envoytherapeutics.com.

Notes

The authors declare no competing financial interest.

Biography

Stephen Hitchcock is Senior Vice President of Drug Discovery at Envoy Therapeutics and adjunct Professor at The Scripps Research Institute, Florida. Between 1994 and 2010, he held senior leadership positions at Eli Lilly and then Amgen. He received a Ph.D. degree in organic chemistry from Nottingham University and then completed a NATO postdoctoral fellowship at Yale University. During his career, he has been fortunate to contribute to and lead teams that have developed several clinical development candidates for CNS disorders including Alzheimer's disease and neuropsychiatric indications, in addition to developing PET imaging agents. He is an author and coinventor on over 70 patents, papers, and review articles.

ABBREVIATIONS USE

P-gp, P-glycoprotein; CNS, central nervous system; ATP, adenosine-5'-triphosphate; SLC, solute carrier class; ABC, ATP-binding cassette; MRP, multidrug resistance protein; BCRP, breast cancer resistance protein; BBB, blood-brain barrier; BCSFB, blood-cerebrospinal fluid barrier; OAT, organic anion transporter; MDR, multidrug resistance protein; DDI, drug-drug interaction; SNP, single nucleotide polymorphism; PXR, pregnane X receptor; SXR, SXR steroid and xenobiotic receptor; TASTPM, double mutant APPswxPS1.M146 V; A β , Amyloid β -peptide; MDCK, Madin-Darby canine kidney; LLC-PK, pig-kidney-derived epithelial; A-B, apical-to-basal; B-A, basal-to-apical; ER, efflux ratio; PAMPA, parallel artificial membrane permeability assay; ADMET, absorption, distribution, metabolism, excretion, and toxicity; logP, logarithm of the octanol/water partition coefficient; clogP, calculated logP; logD, logarithm of the octanol/water distribution coefficient at a given pH; clogD, calculated logD; MW, molecular weight; HBD, hydrogen bond donors; HBA, hydrogen bond acceptors; PSA, polar surface area; tPSA, topological polar surface area; B/P, brain-to-plasma ratio; QSAR, quantitative structure-activity relationship; GPCR, G-protein coupled receptor; hERG, human ether-à-go-go related gene; CFA, complete Freund's adjuvant; WT, wild-type; KO, knockout; BACE, β -Amyloid cleaving enzyme; TS, hydroxyethylamine (HEA) transition state; HIV, human immunodeficiency virus; po, per oral; sc, subcutaneous; ip, intraperitoneal; FDA, Food and Drug Administration; LE, ligand efficiency; cGMP, cyclic guanosine monophosphate

REFERENCES

- (1) Feng, B.; Mills, J. B.; Davidson, R. E.; Mireles, R. J.; Janiszewski, J. S.; Troutman, M. D.; de Moraes, S. M. In vitro P-glycoprotein assays to predict the in vivo interactions of P-glycoprotein with drugs in the central nervous system. *Drug Metab. Dispos.* **2008**, *36*, 268–275.
- (2) Doan, K. M.; M. Humphreys, J. E.; Webster, L. O.; Wring, S. A.; Shampine, L. J.; Serabjit-Singh, C. J.; Adkison, K. K.; Polli, J. W. Passive permeability and P-glycoprotein-mediated efflux differentiate central nervous system (CNS) and non-CNS marketed drugs. *J. Pharmacol. Exp. Ther.* **2002**, *303*, 1029–1037.
- (3) Doran, A.; Obach, R. S.; Smith, B. J.; Hosea, N. A.; Becker, S.; Callegari, E.; Chen, C.; Chen, X.; Choo, E.; Cianfrogna, J.; Cox, L. M.; Gibbs, J. P.; Gibbs, M. A.; Hatch, H.; Hop, C. E. C. A.; Kasman, I. N.; LaPerle, J.; Liu, J.; Liu, X.; Logman, M.; Maclin, D.; Nedza, F. M.; Nelson, F.; Olson, E.; Rahematpura, S.; Raunig, D.; Rogers, S.; Schmidt, K.; Spracklin, D. K.; Szewc, M.; Troutman, M.; Tseng, E.; Tu, M.; Van Deusen, J. W.; Venkatakrisnan, K.; Walens, G.; Wang, E. Q.; Wong, D.; Yasgar, A. S.; Zhang, C. The impact of P-glycoprotein on the disposition of drugs targeted for indications of the central nervous system: evaluation using the MDRIA/1B knockout mouse model. *Drug Metab. Dispos.* **2005**, *33*, 165–174.
- (4) Raub, T. J. P-Glycoprotein recognition of substrates and circumvention through rational drug design. *Mol. Pharmaceutics* **2006**, *3*, 3–25.
- (5) Di, L.; Kerns, E. H.; Bezar, I. F.; Petusky, S. L.; Huang, Y. Comparison of blood-brain barrier permeability assays: in situ brain perfusion, MDR1-MDCKII and PAMPA-BBB. *J. Pharm. Sci.* **2009**, *98*, 1980–1991.
- (6) Schinkel, A. H.; Smit, J. J. M.; van Tellingen, O.; Beijnen, J. H.; Wagenaar, E.; van Deemter, L.; Mol, C. A. A. M.; van der Valk, M. A.; Robanus-Maandag, E. C.; te Riele, H. P. J.; Berns, A. J. M.; Borst, P. Disruption of the mouse *mdr1a* P-glycoprotein gene leads to a deficiency in the blood-brain barrier and to increased sensitivity to drugs. *Cell* **1994**, *77*, 491–502.
- (7) Chen, C.; Liu, X.; Smith, B. J. Utility of *Mdr1*-gene deficient mice in assessing the impact of P-glycoprotein on pharmacokinetics and pharmacodynamics in drug discovery and development. *Curr. Drug Metab.* **2003**, *4*, 272–291.
- (8) Colabufo, N. A.; Berardi, F.; Cantore, M.; Contino, M.; Inglese, C.; Niso, M.; Perrone, R. Perspectives of P-glycoprotein modulating agents in oncology and neurodegenerative diseases: pharmaceutical, biological, and diagnostic potentials. *J. Med. Chem.* **2010**, *53*, 1883–1897.
- (9) Sakaeda, T.; Nakamura, T.; Okumura, K. Pharmacogenetics of drug transporters and its impact on the pharmacotherapy. *Curr. Top. Med. Chem.* **2004**, *4*, 1385–1398.
- (10) Saier, M. H., Jr; Yen, M. R.; Noto, K.; Tamang, D. G.; Elkan, C. The Transporter Classification Database: recent advances. *Nucleic Acids Res.* **2009**, *37*, D274–278.
- (11) Dean, M.; Rzhetsky, A.; Allikmets, R. The human ATP-binding cassette (ABC) transporter superfamily. *Genome Res.* **2001**, *11*, 1156–1166.
- (12) Juliano, R. L.; Ling, V. A surface glycoprotein modulating drug permeability in Chinese hamster ovary cell mutants. *Biochim. Biophys. Acta* **1976**, *455*, 152–162.
- (13) Bauer, B.; Hartz, A. M. S.; Fricker, G.; Miller, D. S. Modulation of p-glycoprotein transport function at the blood-brain barrier. *Exp. Biol. Med.* **2005**, *230*, 118–127.
- (14) Ameyaw, M. M.; Regateiro, F.; Li, T.; Liu, X.; Tariq, M.; Mobarek, A.; Thornton, N.; Folyan, G. O.; Githang'a, J.; Indalo, A.; Ofori-Adjei, D.; Price-Evans, D. A.; McLeod, H. L. MDR1 pharmacogenetics: frequency of the C3435T mutation in exon 26 is significantly influenced by ethnicity. *Pharmacogenetics* **2001**, *11*, 217–221.
- (15) Drożdżik, M.; Białecka, M.; Myśliwiec, K.; Honczarenko, K.; Stankiewicz, J.; Sych, Z. Polymorphism in the P-glycoprotein drug transporter MDR1 gene: a possible link between environmental and genetic factors in Parkinson's disease. *Pharmacogenetics* **2003**, *13*, 259–263.

- (16) Callaghan, R.; Crowley, E.; Potter, S.; Kerr, I. D. P-glycoprotein: So many ways to turn it on. *J. Clin. Pharmacol.* **2008**, *48*, 365–378.
- (17) Bauer, B.; Hartz, A. M. S.; Fricker, G.; Miller, D. S. Pregnane X receptor up-regulation of P-glycoprotein expression and transport function at the blood-brain barrier. *Mol. Pharmacol.* **2004**, *66*, 413–419.
- (18) Bauer, B.; Yang, X.; Hartz, A. M. S.; Olson, E. R.; Zhao, R.; Kalvass, J. C.; Pollack, G. M.; Miller, D. S. In vivo activation of human pregnane X receptor tightens the blood-brain barrier to methadone through P-glycoprotein up-regulation. *Mol. Pharmacol.* **2006**, *70*, 1212–1219.
- (19) Linnert, K.; Ejsing, T. B. A review on the impact of P-glycoprotein on the penetration of drugs into the brain. Focus on psychotropic drugs. *Eur. Neuropsychopharm.* **2008**, *18*, 157–169.
- (20) Remy, S.; Beck, H. Molecular and cellular mechanisms of pharmacoresistance in epilepsy. *Brain* **2006**, *129*, 18–35.
- (21) Löscher, W.; Potschka, H. Drug resistance in brain diseases and the role of drug efflux transporters. *Nat. Rev. Neurosci.* **2005**, *6*, 591–602.
- (22) Aquilante, C. L.; Letrent, S. P.; Pollack, G. M.; Brouwer, K. L. R. Increased brain P-glycoprotein in morphine tolerant rats. *Life Sci.* **1999**, *66*, PL47–PL51.
- (23) Seelbach, M. J.; Brooks, T. A.; Egleton, R. D.; Davis, T. P. Peripheral inflammatory hyperalgesia modulates morphine delivery to the brain: a role for P-glycoprotein. *J. Neurochem.* **2007**, *102*, 1677–1690.
- (24) Cheng, Z.; Zhang, J.; Liu, H.; Li, Y.; Zhao, Y.; Yang, E. Central nervous system penetration for small molecule therapeutic agents does not increase in multiple sclerosis- and Alzheimer's disease-related animal models despite reported blood-brain barrier disruption. *Drug Metab. Dispos.* **2010**, *38*, 1355–1361.
- (25) Bartels, A. L.; Kortekaas, R.; Bart, J.; Willemsen, A. T. M.; de Klerk, O. L.; de Vries, J. J.; van Oostrom, J. C. H.; Leenders, K. L. Blood-brain barrier P-glycoprotein function decreases in specific brain regions with aging: a possible role in progressive neurodegeneration. *Neurobiol. Aging* **2009**, *30*, 1818–1824.
- (26) Bartels, A. L.; de Klerk, O. L.; Kortekaas, R.; de Vries, J. J.; Leenders, K. L. 11C-verapamil to assess P-gp function in human brain during aging, depression and neurodegenerative disease. *Curr. Top. Med. Chem.* **2010**, *10*, 1775–1784.
- (27) Vogelgesang, S.; Cascorbi, I.; Schroeder, E.; Pahnke, J.; Kroemer, H. K.; Siegmund, W.; Kunert-Keil, C.; Walker, L. C.; Warzok, R. W. Deposition of Alzheimer's beta-amyloid is inversely correlated with P-glycoprotein expression in the brains of elderly non-demented humans. *Pharmacogenetics* **2002**, *12*, 535–541.
- (28) Brenn, A.; Grube, M.; Peters, M.; Fischer, A.; Jedlitschky, G.; Kroemer, H. K.; Warzok, R. W.; Vogelgesang, S. Beta-amyloid downregulates MDR1-P-glycoprotein (Abcb1) expression at the blood-brain barrier in mice. *Int. J. Alzheimers. Dis.* **2011**, DOI: 10.4061/2011/690121.
- (29) Lee, C. A.; Cook, J. A.; Reyner, E. L.; Smith, D. A. P-glycoprotein related drug interactions: clinical importance and a consideration of disease states. *Expert Opin. Drug Metab. Toxicol.* **2010**, *6*, 603–619.
- (30) Shaffer, C. L. Defining neuropharmacokinetic parameters in CNS drug discovery to determine cross-species pharmacologic exposure-response relationships. *Annu. Rep. Med. Chem.* **2010**, *45*, 55–70.
- (31) Wong, D. F.; Tauscher, J.; Grunder, G. The role of imaging in proof of concept for CNS drug discovery and development. *Neuropsychopharmacology* **2008**, *34*, 187–203.
- (32) Katoh, M.; Suzuyama, N.; Takeuchi, T.; Yoshitomi, S.; Asahi, S.; Yokoi, T. Kinetic analyses for species differences in P-glycoprotein-mediated drug transport. *J. Pharm. Sci.* **2006**, *95*, 2673–2683.
- (33) Syvänen, S.; Lindhe, Ö.; Palner, M.; Kornum, B. R.; Rahman, O.; Långström, B.; Knudsen, G. M.; Hammarlund-Udenaes, M. Species differences in blood-brain barrier transport of three positron emission tomography radioligands with emphasis on P-glycoprotein transport. *Drug Metab. Dispos.* **2009**, *37*, 635–643.
- (34) Polli, J. W.; Wring, S. A.; Humphreys, J. E.; Huang, L.; Morgan, J. B.; Webster, L. O.; Serabjit-Singh, C. S. Rational use of in vitro P-glycoprotein assays in drug discovery. *J. Pharmacol. Exp. Ther.* **2001**, *299*, 620–628.
- (35) Schwab, D.; Fischer, H.; Tabatabaei, A.; Poli, S.; Huwyler, J. Comparison of in vitro P-glycoprotein screening assays: recommendations for their use in drug discovery. *J. Med. Chem.* **2003**, *46*, 1716–1725.
- (36) Kell, D. B.; Dobson, P. D.; Oliver, S. G. Pharmaceutical drug transport: the issues and the implications that it is essentially carrier-mediated only. *Drug Discovery Today* **2011**, *16*, 704–714.
- (37) Liu, X.; Chen, C. Strategies to optimize brain penetration in drug discovery. *Curr. Opin. Drug Discovery Dev.* **2005**, *8*, 505–512.
- (38) Mensch, J.; Melis, A.; Mackie, C.; Verreck, G.; Brewster, M. E.; Augustijns, P. Evaluation of various PAMPA models to identify the most discriminating method for the prediction of BBB permeability. *Eur. J. Pharm. Biopharm.* **2010**, *74*, 495–502.
- (39) Schinkel, A. H.; Mayer, U.; Wagenaar, E.; Mol, C. A. A. M.; van Deemter, L.; Smit, J. J. M.; van der Valk, M. A.; Voordouw, A. C.; Spits, H.; van Tellingen, O.; Zijlmans, J. M.; Fibbe, W. E.; Borst, P. Normal viability and altered pharmacokinetics in mice lacking mdr1-type (drug-transporting) P-glycoproteins. *Proc. Natl. Acad. Sci. U.S.A.* **1997**, *94*, 4028–4033.
- (40) Hyafil, F.; Vergely, C.; Du Vignaud, P.; Grand-Perret, T. In vitro and in vivo reversal of multidrug resistance by GF120918, an acridonecarboxamide derivative. *Cancer Res.* **1993**, *53*, 4595–4602.
- (41) Cutler, L.; Howes, C.; Deeks, N. J.; Buck, T. L.; Jeffrey, P. Development of a P-glycoprotein knockout model in rodents to define species differences in its functional effect at the blood-brain barrier. *J. Pharm. Sci.* **2006**, *95*, 1944–1953.
- (42) Kodaira, H.; Kusuhara, H.; Ushiki, J.; Fuse, E.; Sugiyama, Y. Kinetic analysis of the cooperation of P-glycoprotein (P-gp/Abcb1) and breast cancer resistance protein (Bcrp/Abcg2) in limiting the brain and testis penetration of erlotinib, flavopiridol, and mitoxantrone. *J. Pharmacol. Exp. Ther.* **2010**, *333*, 788–796.
- (43) Liu, X.; Smith, B. J.; Chen, C.; Callegari, E.; Becker, S. L.; Chen, X.; Cianfrogna, J.; Doran, A. C.; Doran, S. D.; Gibbs, J. P.; Hosea, N.; Liu, J.; Nelson, F. R.; Szewc, M. A.; Van Deusen, J. Evaluation of cerebrospinal fluid concentration and plasma free concentration as a surrogate measurement for brain free concentration. *Drug Metab. Dispos.* **2006**, *34*, 1443–1447.
- (44) Kalvass, J. C.; Maurer, T. S.; Pollack, G. M. Use of plasma and brain unbound fractions to assess the extent of brain distribution of 34 drugs: comparison of unbound concentration ratios to in vivo P-glycoprotein efflux ratios. *Drug Metab. Dispos.* **2007**, *35*, 660–666.
- (45) Jeffrey, P.; Summerfield, S. G. Challenges for blood-brain barrier (BBB) screening. *Xenobiotica* **2007**, *37*, 1135–1151.
- (46) Watson, J.; Wright, S.; Lucas, A.; Clarke, K. L.; Viggers, J.; Cheetham, S.; Jeffrey, P.; Porter, R.; Read, K. D. Receptor occupancy and brain free fraction. *Drug Metab. Dispos.* **2009**, *37*, 753–760.
- (47) Dagenais, C.; Avdeef, A.; Tsinman, O.; Dudley, A.; Beliveau, R. P-glycoprotein deficient mouse in situ blood-brain barrier permeability and its prediction using an in combo PAMPA model. *Eur. J. Pharm. Sci.* **2009**, *38*, 121–137.
- (48) Wager, T. T.; Villalobos, A.; Verhoest, P. R.; Hou, X.; Shaffer, C. L. Strategies to optimize the brain availability of central nervous system drug candidates. *Expert Opin. Drug Discovery.* **2011**, *6*, 371–381.
- (49) Gleeson, M. P. Generation of a set of simple, interpretable ADMET rules of thumb. *J. Med. Chem.* **2008**, *51*, 817–834.
- (50) Fridén, M.; Winiwarter, S.; Jerndal, G.; Bengtsson, O.; Wan, H.; Bredberg, U.; Hammarlund-Udenaes, M.; Antonsson, M. Structure-brain exposure relationships in rat and human using a novel data set of unbound drug concentrations in brain interstitial and cerebrospinal fluids. *J. Med. Chem.* **2009**, *52*, 6233–6243.
- (51) Hitchcock, S. A.; Pennington, L. D. Structure-brain exposure relationships. *J. Med. Chem.* **2006**, *49*, 7559–7583.
- (52) Wager, T. T.; Hou, X.; Verhoest, P. R.; Villalobos, A. Moving beyond rules: the development of a central nervous system

multiparameter optimization (CNS MPO) approach to enable alignment of druglike properties. *ACS Chem. Neurosci.* **2010**, *1*, 435–449.

(53) Meanwell, N. A. Improving drug candidates by design: a focus on physicochemical properties as a means of improving compound disposition and safety. *Chem. Res. Toxicol.* **2011**, *24*, 1345–1410.

(54) Aller, S. G.; Yu, J.; Ward, A.; Weng, Y.; Chittaboina, S.; Zhuo, R.; Harrell, P. M.; Trinh, Y. T.; Zhang, Q.; Urbatsch, I. L.; Chang, G. Structure of P-glycoprotein reveals a molecular basis for poly-specific drug binding. *Science* **2009**, *323*, 1718–1722.

(55) Klepsch, F.; Ecker, G. F. Impact of the recent mouse P-glycoprotein structure for structure-based ligand design. *Mol. Inf.* **2010**, *29*, 276–286.

(56) Dolgih, E.; Bryant, C.; Renslo, A. R.; Jacobson, M. P. Predicting binding to P-glycoprotein by flexible receptor docking. *PLoS Comput. Biol.* **2011**, *7*, e1002083.

(57) Demel, M. A.; Schwaha, R.; Krämer, O.; Ettmayer, P.; Haaksma, E. E.; Ecker, G. F. *In silico* prediction of substrate properties for ABC-multidrug transporters. *Expert Opin. Drug Metab. Toxicol.* **2008**, *4*, 1167–1180.

(58) Huang, H.; Player, M. R. Bradykinin B1 receptor antagonists as potential therapeutic agents for pain. *J. Med. Chem.* **2010**, *53*, 5383–5399.

(59) Kuduk, S. D.; Di Marco, C. N.; Chang, R. K.; Wood, M. R.; Schirripa, K. M.; Kim, J. J.; Wai, J. M.; C. DiPardo, R. M.; Murphy, K. L.; Ransom, R. W.; Harrell, C. M.; Reiss, D. R.; Holahan, M. A.; Cook, J.; Hess, J. F.; Sain, N.; Urban, M. O.; Tang, C.; Prueksaritanont, T.; Pettibone, D. J.; Bock, M. G. Development of orally bioavailable and CNS penetrant biphenylaminocyclopropane carboxamide bradykinin B1 receptor antagonists. *J. Med. Chem.* **2007**, *50*, 272–282.

(60) Yuan, Y.; Li, G.; He, H.; Stevens, D. L.; Kozak, P.; Scoggins, K. L.; Mitra, P.; Gerke, P. M.; Selvey, D. E.; Dewey, W. L.; Zhang, Y. Characterization of 6α - and 6β -N-heterocyclic substituted naltrexamine derivatives as novel leads to development of mu opioid receptor selective antagonists. *ACS Chem. Neurosci.* **2011**, *2*, 346–351.

(61) Hyafil, F.; Vergely, C.; Du, V. P.; Grand-Perret, T. In vitro and in vivo reversal of multidrug resistance by GF120918, an acridinecarboxamide derivative. *Cancer Res.* **1993**, *53*, 4595–4602.

(62) Olsen, R. A.; Liu, L.; Ghaderi, N.; Johns, A.; Hatcher, M. E.; Mueller, L. J. The amide rotational barriers in picolinamide and nicotinamide: NMR and ab initio studies. *J. Am. Chem. Soc.* **2003**, *125*, 10125–10132.

(63) Hamada, Y.; Kiso, Y. Recent progress in the drug discovery of non-peptidic BACE1 inhibitors. *Expert Opin. Drug Discovery* **2009**, *4*, 391–416.

(64) Silvestri, R. Boom in the development of non-peptidic β -secretase (BACE1) inhibitors for the treatment of Alzheimer's disease. *Med. Res. Rev.* **2009**, *29*, 295–338.

(65) Varghese, J., Ed. *BACE: Lead Target for Orchestrated Therapy of Alzheimer's Disease*; John Wiley & Sons: New York, 2010.

(66) Varatharajan, L.; Thomas, S. A. The transport of anti-HIV drugs across blood–CNS interfaces: Summary of current knowledge and recommendations for further research. *Antiviral Res.* **2009**, *82*, A99–A109.

(67) Xue, Q.; Albrecht, B. K.; Andersen, D. L.; Bartberger, M.; Brown, J.; Brown, R.; Chaffee, S. C.; Cheng, Y.; Croghan, M.; Graceffa, R.; Harried, S.; Hitchcock, S.; Hungate, R.; Judd, T.; Kaller, M.; Kreiman, C.; La, D.; Lopez, P.; Masse, C. E.; Monenschein, H.; Nguyen, T.; Nixey, T.; Patel, V. F.; Pennington, L.; Weiss, M.; Yang, B.; Zhong, W. Preparation of 2-Hydroxy-1,3-diaminoalkanes including Spiro Substituted Chroman Derivatives as β -Secretase Modulators and Their Use for Treatment Alzheimer's Disease and Related Condition. PCT Intl. Appl. WO2007061930.

(68) Hitchcock, S.; Orally Active, Brain Penetrant Beta-Secretase (BACE) Inhibitors: Consolidating Property-Based and Structure-Based Drug Design. 3rd International Symposium on Advances in Synthetic and Medicinal Chemistry, Kiev, Ukraine, August 23, 2009.

(69) Hennig, L.; Ayala-Leon, K.; Angulo-Cornejo, J.; Richter, R.; Beyer, L. Fluorine hydrogen short contacts and hydrogen bonds in substituted benzamides. *J. Fluorine Chem.* **2009**, *130*, 453–460.

(70) Fritz, H.; Winkler, T. Weitreichende kopplung zwischen protonen und fluor in 2-fluorbenzamidin. *Helv. Chim. Acta* **1974**, *57*, 836–839.

(71) Ward, S. E.; Harries, M.; Aldegheri, L.; Andreotti, D.; Ballantine, S.; Bax, B. D.; Harris, A. J.; Harker, A. J.; Lund, J.; Melarange, R.; Mingardi, A.; Mookherjee, C.; Mosley, J.; Neve, M.; Oliosi, B.; Profeta, R.; Smith, K. J.; Smith, P. W.; Spada, S.; Thewlis, K. M.; Yusuf, S. P. Discovery of N-[(2S)-5-(6-fluoro-3-pyridinyl)-2,3-dihydro-1H-inden-2-yl]-2-propanesulfonamide, a novel clinical AMPA receptor positive modulator. *J. Med. Chem.* **2010**, *53*, S801–S812.

(72) Shi, F.; Shen, J. K.; Chen, D.; Fog, K.; Thirstrup, K.; Hentzer, M.; Karlsson, J.-J.; Menon, V.; Jones, K. A.; Smith, K. E.; Smith, G. Discovery and SAR of a series of agonists at orphan G protein-coupled receptor 139. *ACS Med. Chem. Lett.* **2011**, *2*, 303–306.

(73) Wakenhut, F.; Allan, G. A.; Fish, P. V.; Jonathan Fray, M.; Harrison, A. C.; McCoy, R.; Phillips, S. C.; Stobie, A.; Westbrook, D.; Westbrook, S. L.; Whitlock, G. A. N-[(3S)-Pyrrolidin-3-yl]benzamides as novel dual serotonin and noradrenergic reuptake inhibitors: Impact of small structural modifications on P-gp recognition and CNS penetration. *Bioorg. Med. Chem. Lett.* **2009**, *19*, 5078–5081.

(74) Hughes, J. D.; Blegg, J.; Price, D. A.; Bailey, S.; DeCrescenzo, G. A.; Devraj, R. V.; Ellsworth, E.; Fobian, Y. M.; Gibbs, M. E.; Gilles, R. W.; Greene, N.; Huang, E.; Krieger-Burke, T.; Loesel, J.; Wager, T.; Whiteley, L.; Zhang, Y. Physicochemical drug properties associated with in vivo toxicological outcomes. *Bioorg. Med. Chem. Lett.* **2008**, *18*, 4872–4875.

(75) Bergman, J. M.; Roecker, A. J.; Mercer, S. P.; Bednar, R. A.; Reiss, D. R.; Ransom, R. W.; Meacham Harrell, C.; Pettibone, D. J.; Lemaire, W.; Murphy, K. L.; Li, C.; Prueksaritanont, T.; Winrow, C. J.; Renger, J. J.; Koblan, K. S.; Hartman, G. D.; Coleman, P. J. Proline bis-amides as potent dual orexin receptor antagonists. *Bioorg. Med. Chem. Lett.* **2008**, *18*, 1425–1430.

(76) Giblin, G. M. P.; Billinton, A.; Briggs, M.; Brown, A. J.; Chessell, I. P.; Clayton, N. M.; Eatherton, A. J.; Goldsmith, P.; Haslam, C.; Johnson, M. R.; Mitchell, W. L.; Naylor, A.; Perboni, A.; Slingsby, B. P.; Wilson, A. W. Discovery of 1-[4-(3-chlorophenylamino)-1-methyl-1H-pyrrolo[3,2-c]pyridin-7-yl]-1-morpholin-4-ylmethanone (GSK554418A), a brain penetrant 5-azaindole CB2 agonist for the treatment of chronic pain. *J. Med. Chem.* **2009**, *52*, 5785–5788.

(77) Verhoest, P. R.; Sawant Basak, A.; Parikh, V.; Hayward, M.; Kauffman, G. W.; Paradis, V.; McHardy, S. F.; McLean, S.; Grimwood, S.; Schmidt, A. W.; Vanase-Frawley, M.; Freeman, J.; Van Deusen, J.; Cox, L.; Wong, D.; Liras, S. Design and discovery of a selective small molecule κ opioid antagonist (2-methyl-N-((2'-(pyrrolidin-1-yl)sulfonyl)biphenyl-4-yl)methyl)propan-1-amine, PF-4455242. *J. Med. Chem.* **2011**, *54*, 5868–5877.

(78) Dosaka-Akita, K.; Tortella, F. C.; Holaday, J. W.; Long, J. B. The kappa opioid agonist U-50488H antagonizes respiratory effects of mu opioid receptor agonists in conscious rats. *J. Pharmacol. Exp. Ther.* **1993**, *264*, 631–637.

(79) Su, D.-S.; Lim, J. L.; Tinney, E.; Wan, B.-L.; Murphy, K. L.; Reiss, D. R.; Harrell, C. M.; O'Malley, S. S.; Ransom, R. W.; Chang, R. S. L.; Pettibone, D. J.; Yu, J.; Tang, C.; Prueksaritanont, T.; Freidinger, R. M.; Bock, M. G.; Anthony, N. J. *J. Med. Chem.* **2008**, *51*, 3946–3952.

(80) Cox, C. D.; Breslin, M. J.; Whitman, D. B.; Coleman, P. J.; Garbaccio, R. M.; Fraley, M. E.; Zrada, M. M.; Buser, C. A.; Walsh, E. S.; Hamilton, K.; Lobell, R. B.; Tao, W.; Abrams, M. T.; South, V. J.; Huber, H. E.; Kohl, N. E.; Hartman, G. D. Kinesin spindle protein (KSP) inhibitors. Part V: discovery of 2-propylamino-2,4-diaryl-2,5-dihydropyrrololes as potent, water-soluble KSP inhibitors, and modulation of their basicity by beta-fluorination to overcome cellular efflux by P-glycoprotein. *Bioorg. Med. Chem. Lett.* **2007**, *17*, 2697–2702.

(81) Guo, Q.; Chandrasekhar, J.; Ihle, D.; Wustrow, D. J.; Chenard, B. L.; Krause, J. E.; Hutchison, A.; Alderman, D.; Cheng, C.; Cortright,

D.; Broom, D.; Kershaw, M. T.; Simmermacher-Mayer, J.; Peng, Y.; Hodgetts, K. J. 1-Benzylbenzimidazoles: the discovery of a novel series of bradykinin B(1) receptor antagonists. *Bioorg. Med. Chem. Lett.* **2008**, *18*, 5027–5031.

(82) Chen, C.; Hanson, E.; Watson, J. W.; Lee, J. S. P-glycoprotein limits the brain penetration of non-sedating but not sedating H1-antagonists. *Drug Metab. Dispos.* **2003**, *31*, 312–318.

(83) Broccatelli, F.; Carosati, E.; Cruciani, G.; Oprea, T. I. Transporter-mediated efflux influences CNS side effects: ABCB1, from antitarget to target. *Mol. Inf.* **2010**, *29*, 16–26.

(84) Nagase, T.; Mizutani, T.; Ishikawa, S.; Sekino, E.; Sasaki, T.; Fujimura, T.; Ito, S.; Mitobe, Y.; Miyamoto, Y.; Yoshimoto, R.; Tanaka, T.; Ishihara, A.; Takenaga, N.; Tokita, S.; Fukami, T.; Sato, N. Synthesis, structure-activity relationships, and biological profiles of a quinazolinone class of histamine H3 receptor inverse agonists. *J. Med. Chem.* **2008**, *51*, 4780–4789.

(85) L. Mercer, S.; Coop, A. Opioid analgesics and P-glycoprotein efflux transporters: a potential systems-level contribution to analgesic tolerance. *Curr. Top. Med. Chem.* **2011**, *11*, 1157–1164.

(86) Cunningham, C. W.; Mercer, S. L.; Hassan, H. E.; Traynor, J. R.; Eddington, N. D.; Coop, A. Opioids and efflux transporters. Part 2: P-glycoprotein substrate activity of 3- and 6-substituted morphine analogs. *J. Med. Chem.* **2008**, *51*, 2316–2320.

(87) Mahar Doan, K. M.; Wring, S. A.; Shampine, L. J.; Jordan, K. H.; Bishop, J. P.; Kratz, J.; Yang, E.; Serabjit-Singh, C. J.; Adkison, K. K.; Polli, J. W. Steady-state brain concentrations of antihistamines in rats: interplay of membrane permeability, P-glycoprotein efflux and plasma protein binding. *Pharmacology* **2004**, *72*, 92–98.

(88) Zhao, R.; Kalvass, J. C.; Yanni, S. B.; Bridges, A. S.; Pollack, G. M. Fexofenadine brain exposure and the influence of blood-brain barrier P-glycoprotein after fexofenadine and terfenadine administration. *Drug Metab. Dispos.* **2009**, *37*, 529–535.

(89) Helal, C. J.; Kang, Z.; Hou, X.; Pandit, J.; Chappie, T. A.; Humphrey, J. M.; Marr, E. S.; Fennell, K. F.; Chenard, L. K.; Fox, C.; Schmidt, C. J.; Williams, R. D.; Chapin, D. S.; Siuciak, J.; Lebel, L.; Menniti, F.; Cianfrogna, J.; Fonseca, K. R.; Nelson, F. R.; O'Connor, R.; Macdougall, M.; McDowell, L.; Liras, S. Use of structure-based design to discover a potent, selective, in vivo active phosphodiesterase 10A inhibitor lead series for the treatment of schizophrenia. *J. Med. Chem.* **2011**, *54*, 4536–4547.

(90) Swinney, D. C.; Anthony, J. How were new medicines discovered? *Nat. Rev. Drug Discovery* **2011**, *10*, 507–519.

(91) Conn, J. P.; Christopoulos, A.; Lindsley, C. W. Allosteric modulators of GPCRs: a novel approach for the treatment of CNS disorders. *Nat. Rev. Drug Discovery* **2009**, *8*, 41–54.